

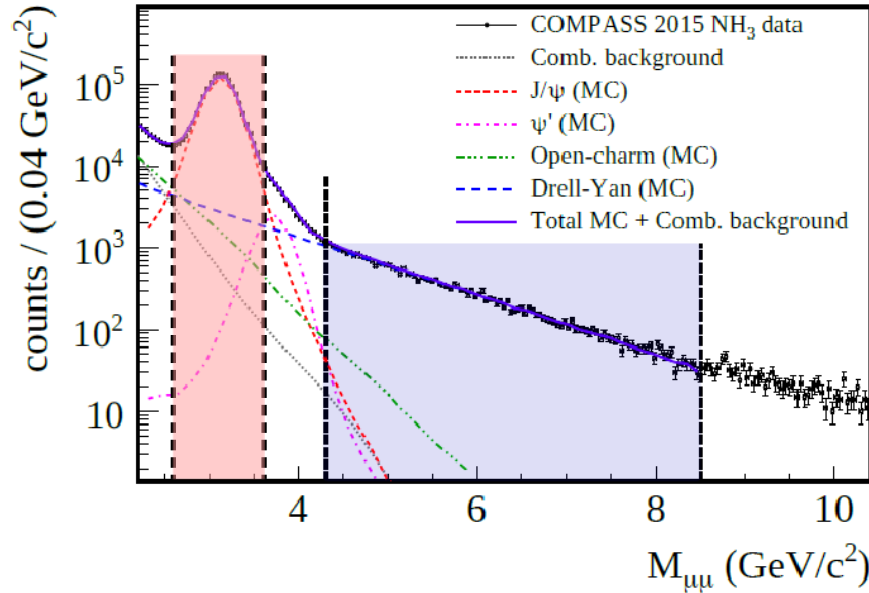
# Drell-Yan and charmonium results from COMPASS

Catarina Quintans, LIP-Lisbon  
on behalf of the COMPASS Collaboration

Mass in Huelva, 09/01/2025



# Goals of the COMPASS Drell-Yan programme



## Pion-induced Drell-Yan:

- Transversely polarized target (NH3)
- Unpolarized targets (NH3+He; Al; W)

## Charmonium production:

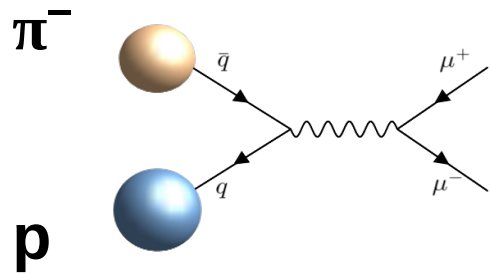
- Cross section
- Polarization
- J/psi pair production

- ➔ Studies of the transversely polarized TMD PDFs of the nucleon, complementary to SIDIS ones.
- ➔ Unique access to the (TMD) PDFs of the pion.
- ➔ Charmonium production at intermediate energies – study of production mechanisms.

# COMPASS Drell-Yan measurement

Drell-Yan cross section:

$$\sigma_{\pi p} = \sum_{a,b} \int_0^1 dx_\pi dx_N f_a(x_N, \mu_F^2) f_b(x_\pi, \mu_f^2) \hat{\sigma}_{ab}$$



The sum is over all parton interactions a,b (q,  $\bar{q}$ , g)

$\hat{\sigma}_{ab}$  are the partonic cross sections, calculable

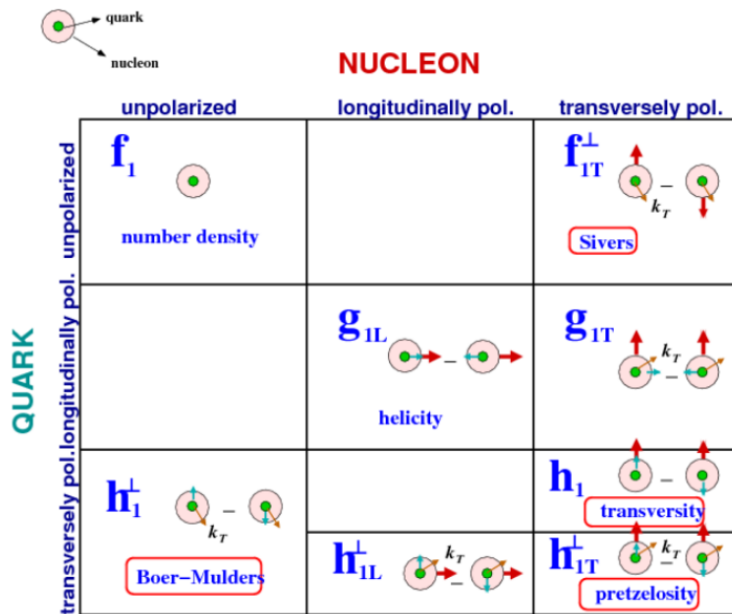
$f_{a,b}$  are the parton distribution functions from beam and target.

The cross section can be interpreted in terms of:

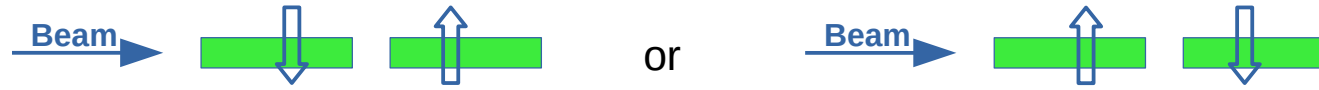
- $f_{a,b}(x_{N,\pi}, \mu_f^2) \rightarrow$  **PDFs**
- $f_{a,b}(x_{N,\pi}, k_T, \mu_f^2) \rightarrow$  **TMD PDFs**

3 collinear PDFs used to describe the proton and its dependences (x,  $Q^2$ ):  
Unpolarized; Helicity; Transversity.

If considering also the transverse motion, at leading twist  
8 quark TMD PDFs are needed to describe the proton (x,  $k_T$ ,  $Q^2$ ).



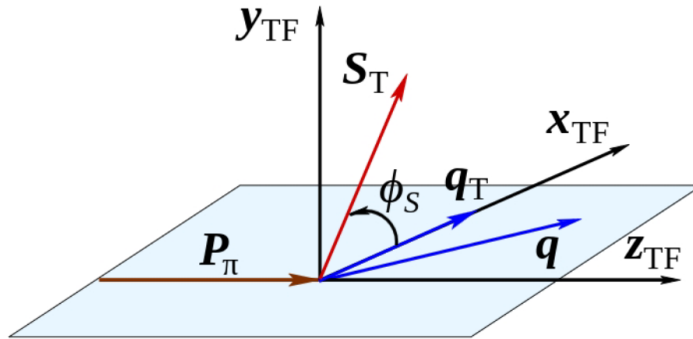
# Spin Asymmetries



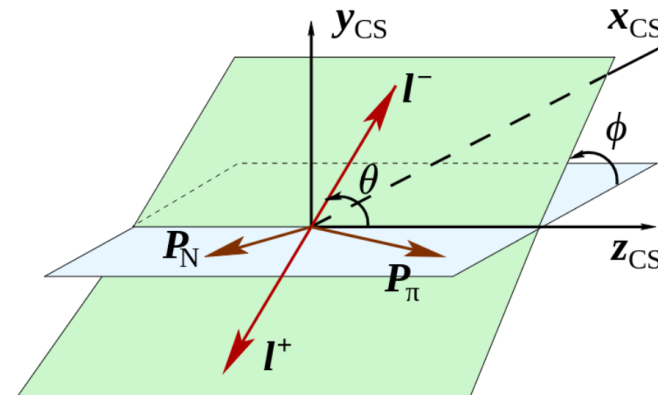
Transversely polarized target in 2 different spin configurations

$$\text{Asymmetry} = \frac{\sigma^{\uparrow\downarrow} - \sigma^{\downarrow\uparrow}}{\sigma^{\uparrow\downarrow} + \sigma^{\downarrow\uparrow}}$$

## Target rest frame



## Collins-Soper frame



# Transverse Momentum Dependent PDFs

## Sivers and the expected sign-change between SIDIS and DY

- Sivers function**: if non-zero then orbital angular momentum is non-vanishing
- Sivers** and **Boer-Mulders** are time-reversal odd: opportunity for a crucial test of the TMD approach of QCD ( $q_T \ll Q$ ):

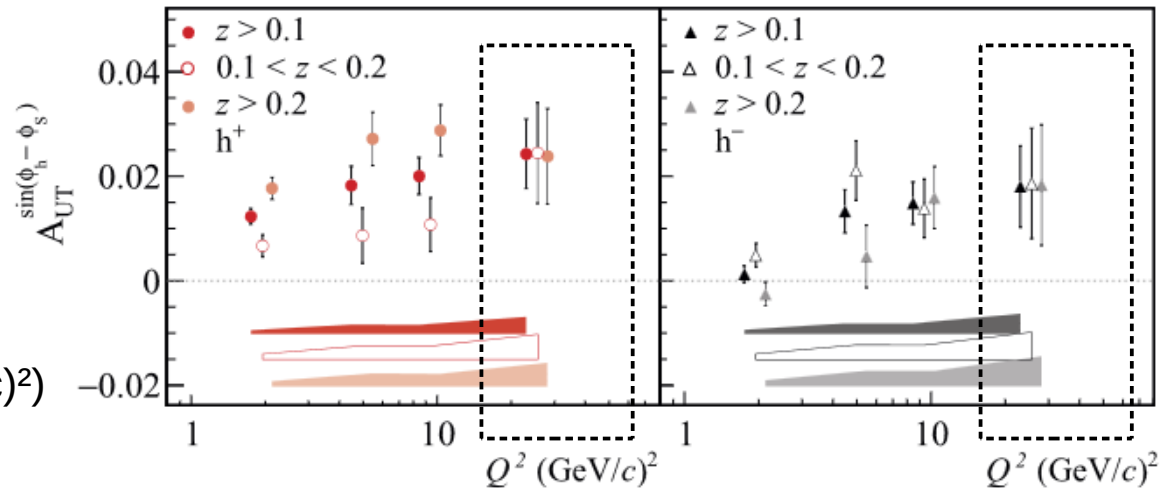
$$h_1^\perp (\text{SIDIS}) = - h_1^\perp (\text{DY})$$

$$f_{1T}^\perp (\text{SIDIS}) = - f_{1T}^\perp (\text{DY})$$

In Drell-Yan,  $q_T$  is the transverse momentum of the final state dimuon, while  $Q$  is the dimuon invariant mass.

COMPASS **Sivers asymmetry** in **SIDIS**:  
PLB 770 (2017) 138-145

-----> Measured in a range common to Drell-Yan ( $16 < Q^2 < 81 \text{ (GeV/c)}^2$ )





# Drell-Yan measurements at COMPASS

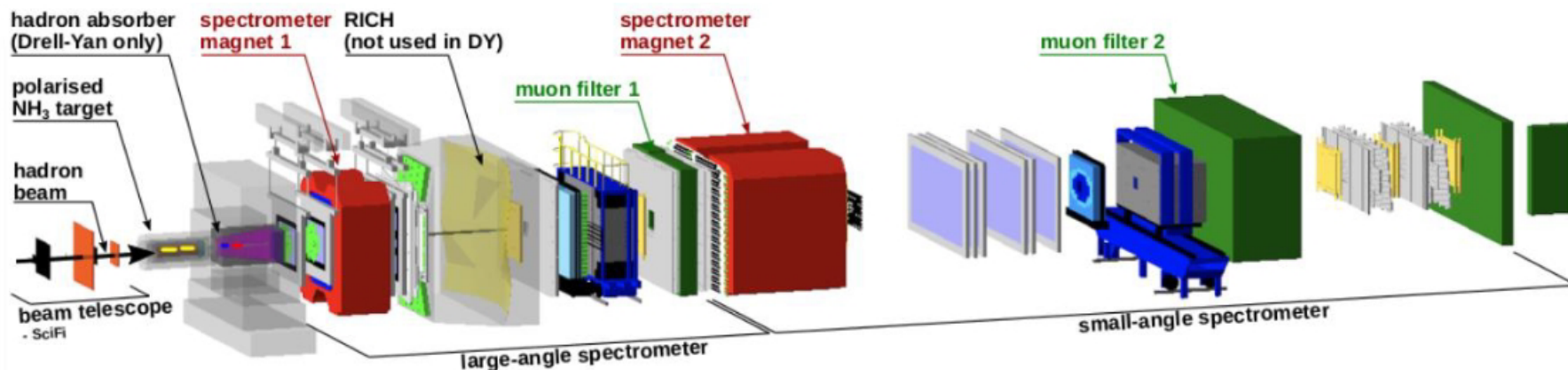
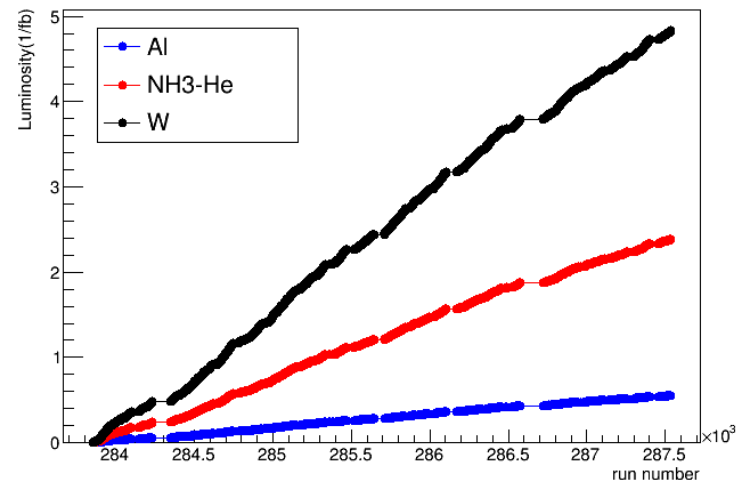
At the M2 beamline @ CERN

Negative hadron beam, 190 GeV/c:

- 96.8%  $\pi^-$
- 2.4%  $K^-$
- $< 1\%$   $\bar{p}$

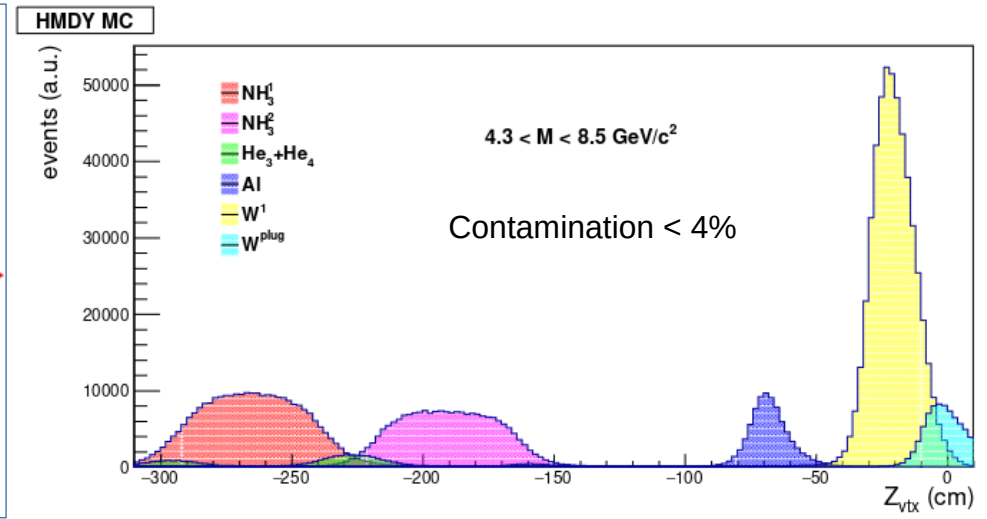
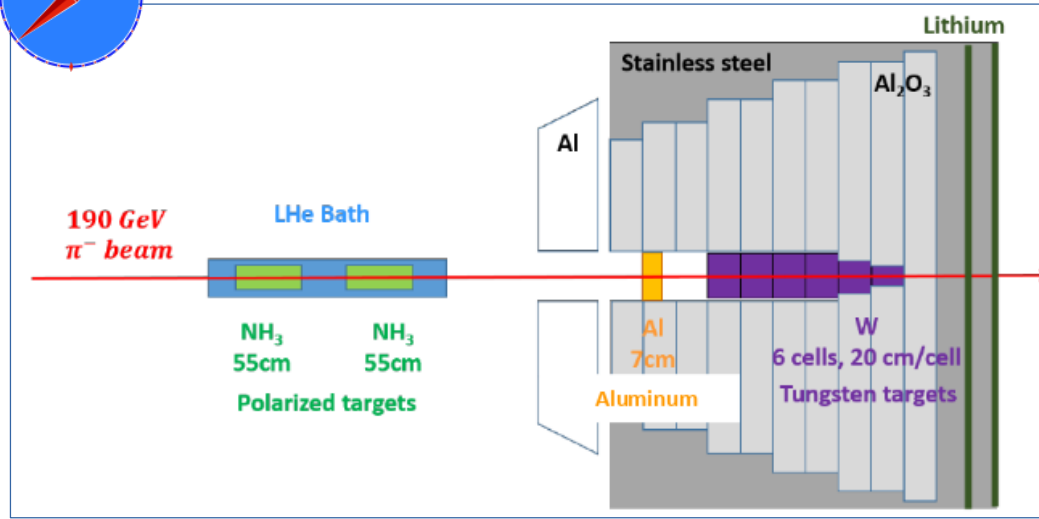
No beam PID. All beam is considered as pions, beam contamination accounted for in the systematics for  $\pi$ -induced Drell-Yan cross section.

2018 integrated luminosity, per target



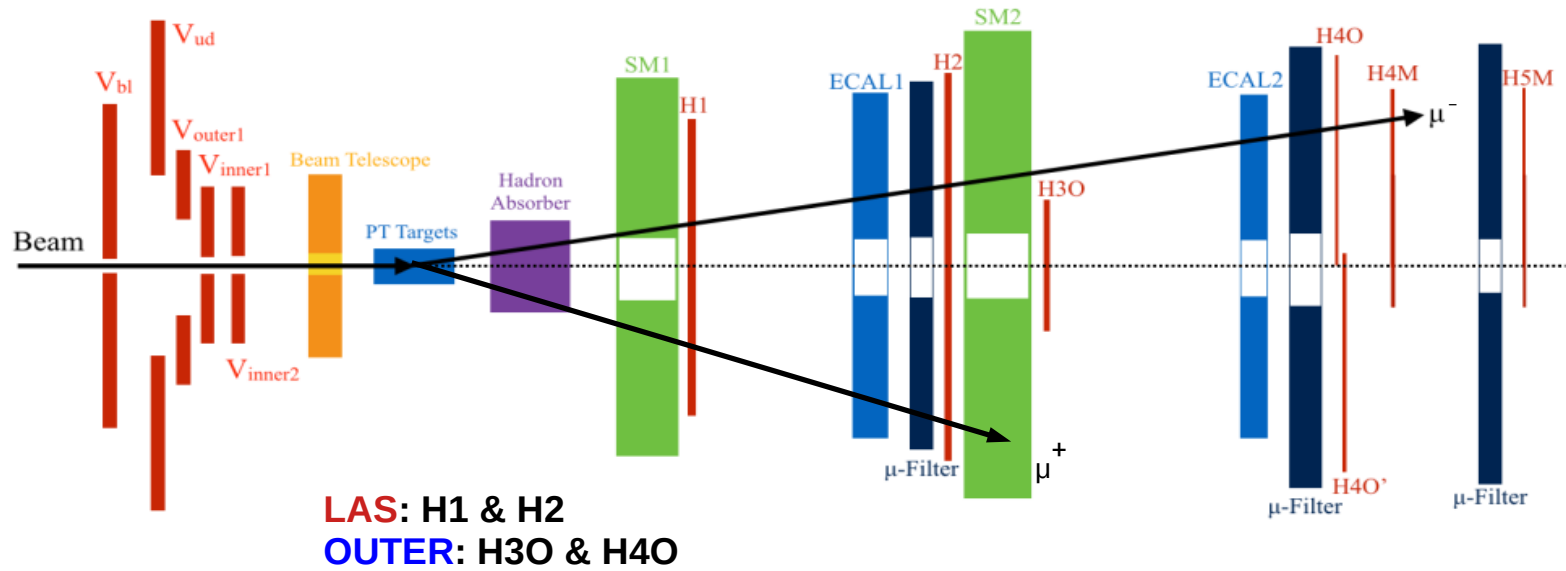


# COMPASS targets



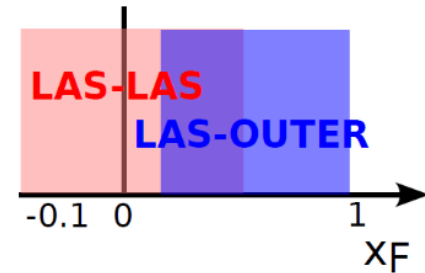
- Transversely polarized target: a mixture of NH<sub>3</sub> beads immersed in He.
- The 2 ammonia target cells are oppositely polarized.
- Spin asymmetries are sensitive to the polarizable part only: roughly, the 3 protons in the hydrogen from NH<sub>3</sub>
- The sum of events from both ammonia cells over the entire year is effectively unpolarized.
- In absolute cross section measurement, all nucleons contribute: for the ammonia mix, consider the molar fractions:  
15.7 % H, 11.1 % <sup>4</sup>He, 73.2 % <sup>14</sup>N
- The contamination from other materials into the considered volumes for each target is <4% .

# Dimuon trigger system



2 triggers, based on the time coincidence of hodoscope pairs:

- 2 muons emitted at large angle (**LAS-LAS**)
- 1 muon at large angle, 1 muon at small angle (**LAS-OUTER**)





# Transverse Spin Asymmetries from DY



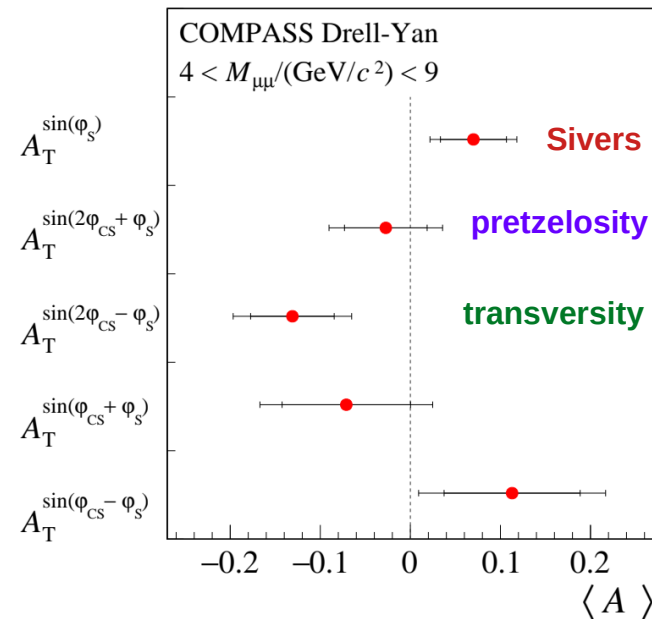
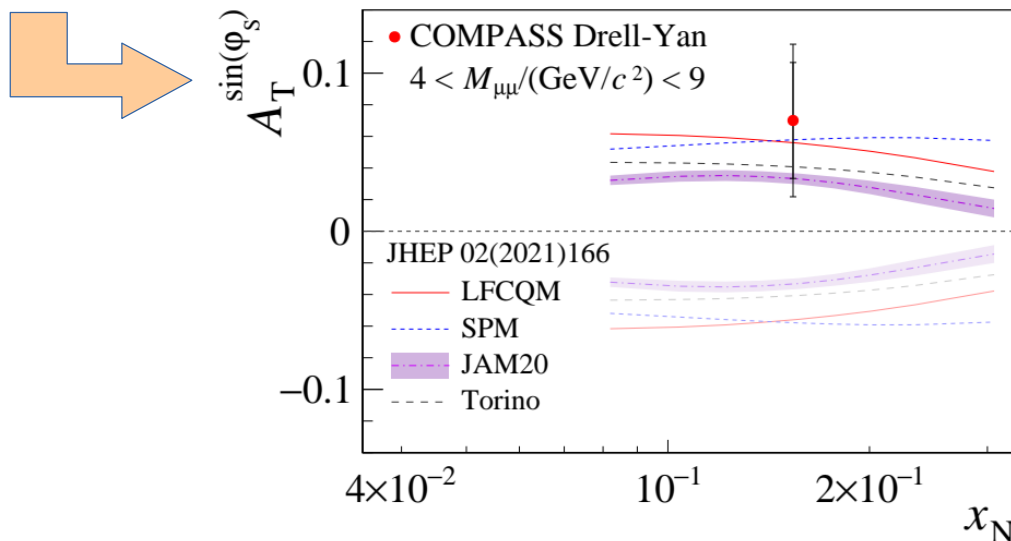
Final results now in: PRL 133 (2024) 071902

Extended mass range: 4 – 9 GeV/c<sup>2</sup>. Contamination from other processes is taken into account as a dilution effect to the asymmetries.

Theory curves based on S. Bastami et al, JHEP 02 (2021) 166.

Sivers asymmetry in SIDIS measured by COMPASS, with nearly same spectrometer, and also in the same Q<sup>2</sup> range.

Data favors the sign change scenario of the Sivers TMD PDF, between SIDIS and DY



These asymmetries relate to convolutions of the TMD PDFs:

$$A_T^{\sin(\phi_S)} \propto \tilde{f}_1^\pi(x_\pi, k_{T,\pi}) \otimes f_{1T}^{\perp,p}(x_N, k_{T,p})$$

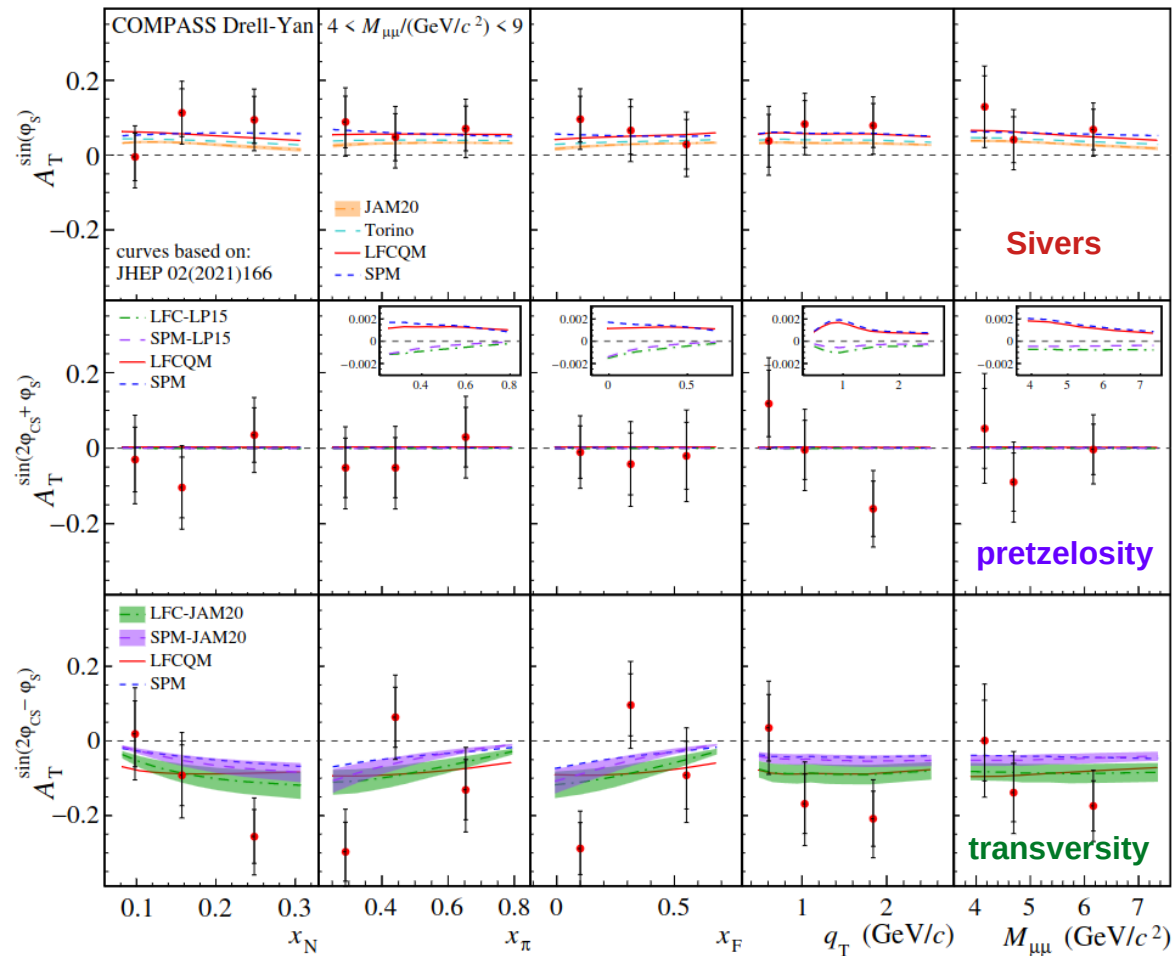
$$A_T^{\sin(2\phi + \phi_S)} \propto \bar{h}_1^{\perp,\pi}(x_\pi, k_{T,\pi}) \otimes h_{1T}^{\perp,p}(x_N, k_{T,p})$$

$$A_T^{\sin(2\phi - \phi_S)} \propto \bar{h}_1^{\perp,\pi}(x_\pi, k_{T,\pi}) \otimes h_1^p(x_N, k_{T,p})$$

# Drell-Yan TSAs (standard)



Final results now in: PRL 133 (2024) 071902



Full data samples: 2015 + 2018

~100K dimuon events, after selection

Extended mass range:  
 $4 < M_{\mu\mu}/(\text{GeV}/c^2) < 9$

Results consistent with first publication  
(based on 2015 data only)  
PRL 119 (2017) 112002.

# $q_T$ -weighted transverse Spin Asymmetries from DY



With respect to the standard analysis, it has the advantage of giving direct access to the n-th moments of the TMD PDFs:

**Standard**

$$A_T^{\sin(\phi_S)} \propto \tilde{f}_1^\pi \otimes f_{1T}^{\perp, p}$$

$$A_T^{\sin(2\phi + \phi_S)} \propto \bar{h}_1^{\perp, \pi} \otimes h_{1T}^{\perp, p}$$

$$A_T^{\sin(2\phi - \phi_S)} \propto \bar{h}_1^{\perp, \pi} \otimes h_1^p$$

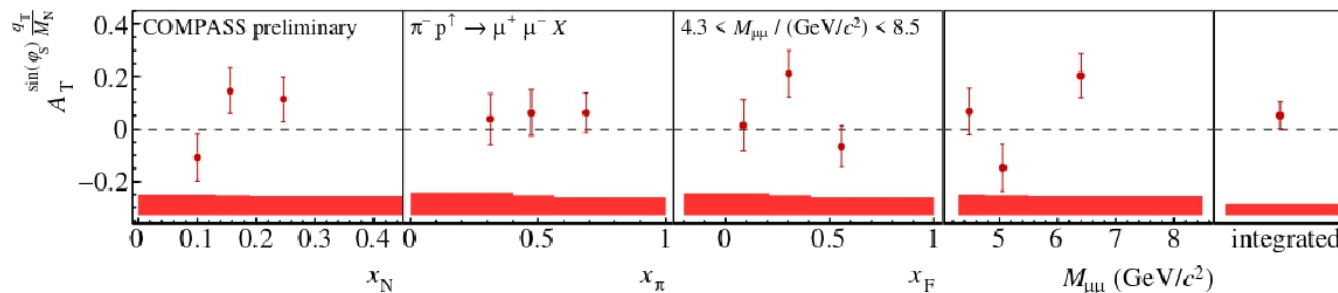
**$q_T$ -weighted**

$$A_T^{\sin(\phi_S) q_T/M_N} \propto \tilde{f}_1^\pi \times f_{1T}^{\perp(1), p}$$

$$A_T^{\sin(2\phi + \phi_S) q_T^3/M_N^2/M_\pi} \propto \bar{h}_1^{\perp(1), \pi} \times h_{1T}^{\perp(2), p}$$

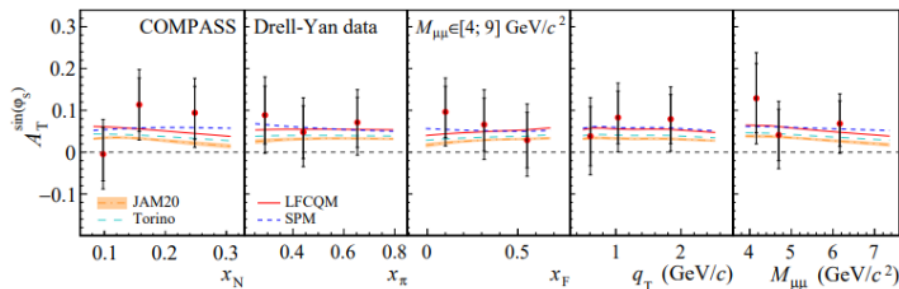
$$A_T^{\sin(2\phi - \phi_S) q_T/M_\pi} \propto \bar{h}_1^{\perp(1), \pi} \times h_1^p$$

**Sivers  $q_T$ -weighted**



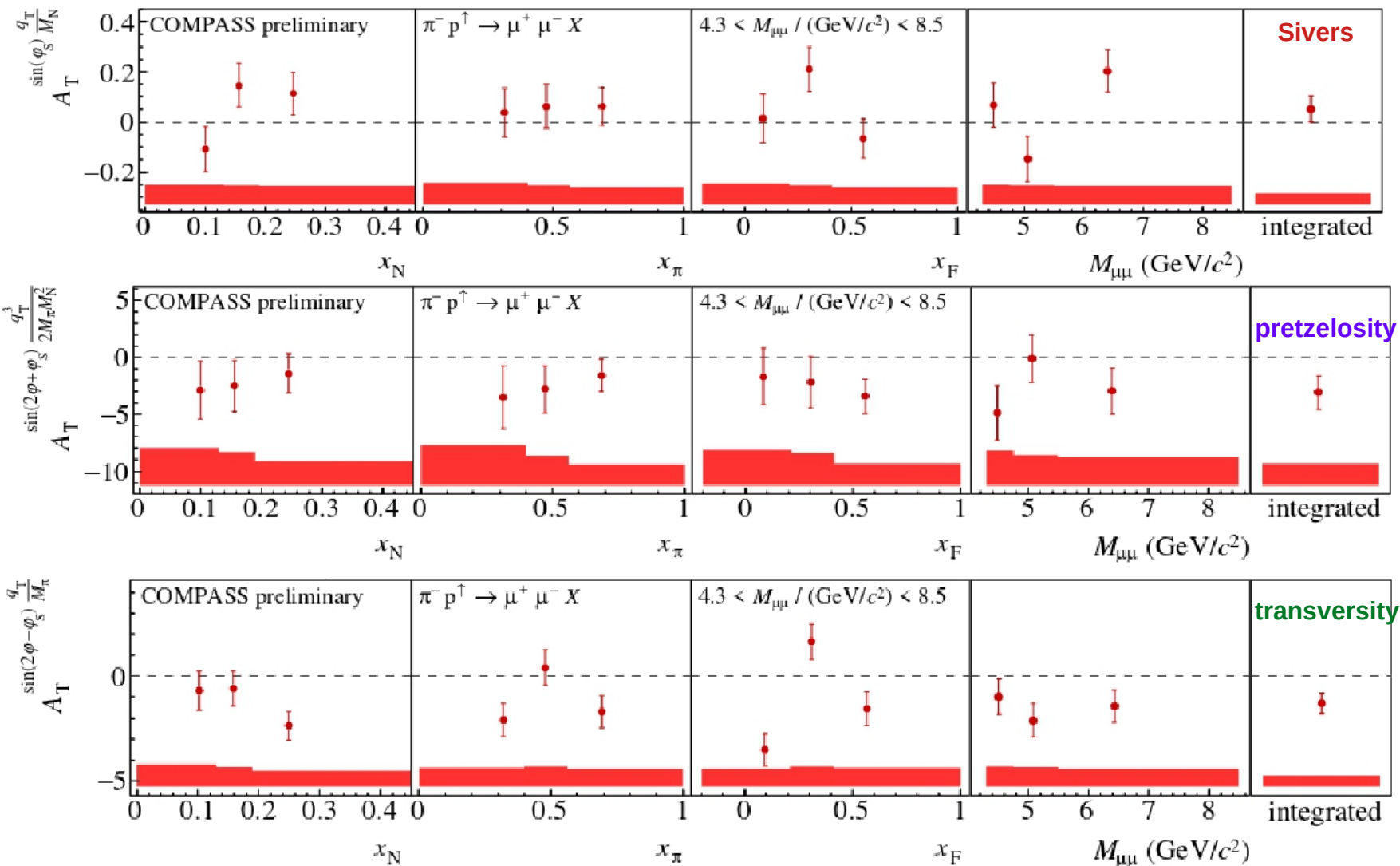
**Sivers TSA (standard)**

(PRL 133 (2024) 071902)



$1\sigma$  positive Sivers WTSA,  
compatibility TSA  $\leftrightarrow$  WTSA

# Drell-Yan $q_T$ -weighted TSAs



$1\sigma$  positive

$2\sigma$  negative

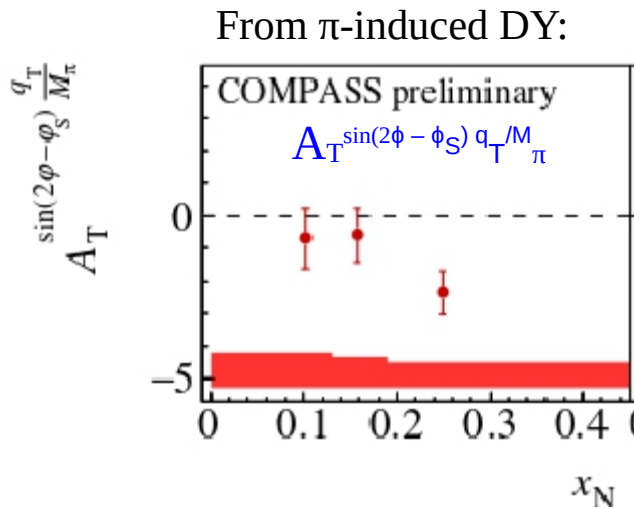
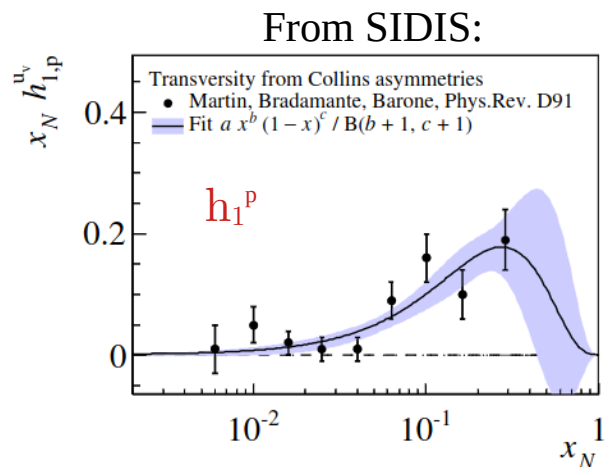
$2\sigma$  negative

# Pion Boer-Mulders TMD PDF: a recipe

Transversity-related WTSA:  $A_T^{\sin(2\phi - \phi_S) q_T/M_\pi} \propto \bar{h}_1^{\perp(1), \pi} \times h_1^p$

$$\approx -2 \frac{e_u^2 h_{1,\pi}^{\perp(1)\bar{u}}(x_\pi) h_{1,p}^u(x_N)}{\sum_{q=u,d,s} e_q^2 [f_{1,\pi}^{\bar{q}}(x_\pi) f_{1,p}^q(x_N) + (q \leftrightarrow \bar{q})]}$$

- $f_1^p$  and  $f_1^\pi$  are the unpolarized TMD PDFs of nucleon and pion, taken from CTEQ5D and GRV-PI, respectively.
- $h_1^p$  is the transversity TMD PDF of the nucleon, interpolated by a simple fit to the Collins asymmetry  
[A. Martin et al, PRD 91 \(2015\) 014034](#)
- $\bar{h}_1^{\perp(1), \pi}$  is 1<sup>st</sup>  $k_T^2$  moment of the Boer-Mulders TMD PDF of the pion.



Access the 1<sup>st</sup> moment of the pion Boer-Mulders

$\bar{h}_1^{\perp(1), \pi}$

# Pion structure

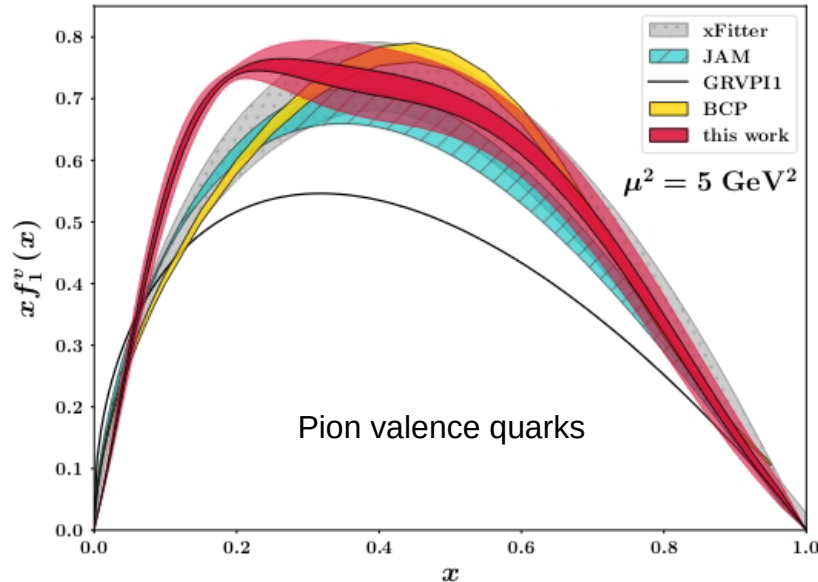
$$\sigma_{\pi p} = \sum_{a,b} \int_0^1 dx_\pi dx_N f_a(x_N, \mu_F^2) f_b(x_\pi, \mu_f^2) \hat{\sigma}_{ab}$$

Pion-induced Drell-Yan provides an access to both proton and pion structure.

In COMPASS Drell-Yan there is mostly sensitivity to the u-quark PDFs in the valence region.

Proton PDFs are known to a good accuracy. Not the case for pion PDFs!

MAP Coll., Phys.Rev.D 107, 114023 (2023)



Available pion-induced DY data is more than 30 years old

Most relevant statistics from E615 (Fermilab) and NA10 (CERN), but using W target – non-negligible nuclear effects.

Very limited information on systematic uncertainties was provided by past experiments.

Only  $\pi^-$  beam, thus little sensitivity to sea quarks.

# Boer-Mulders TMD PDF

The unpolarized Drell-Yan cross section angular dependence gives us also an access to the Boer-Mulders TMD PDFs:

$$\frac{d\sigma}{dq^4 d\Omega} \propto \hat{\sigma}_U \left\{ 1 + A_U^1 \cos^2 \theta_{CS} + \sin 2\theta_{CS} A_U^{\cos \varphi_{CS}} \cos \varphi_{CS} + \sin^2 \theta_{CS} A_U^{\cos 2\varphi_{CS}} \cos 2\varphi_{CS} \right\}$$

**Spin independent**

or

$$\frac{d\sigma}{d\Omega} \propto \frac{3}{4\pi} \frac{1}{\lambda + 3} \left[ 1 + \lambda \cos^2 \theta_{CS} + \mu \sin 2\theta_{CS} \cos \varphi_{CS} + \frac{\nu}{2} \sin^2 \theta_{CS} \cos 2\varphi_{CS} \right]$$

where:  $\lambda = A_U^1$ ,  $\mu = A_U^{\cos \phi}$ ,  $\nu = 2 A_U^{\cos 2\phi}$

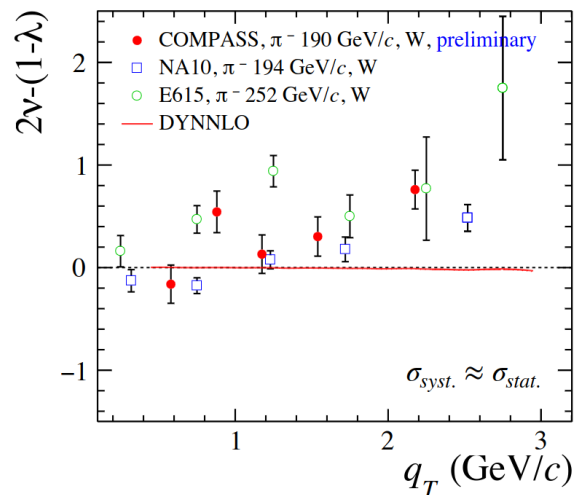
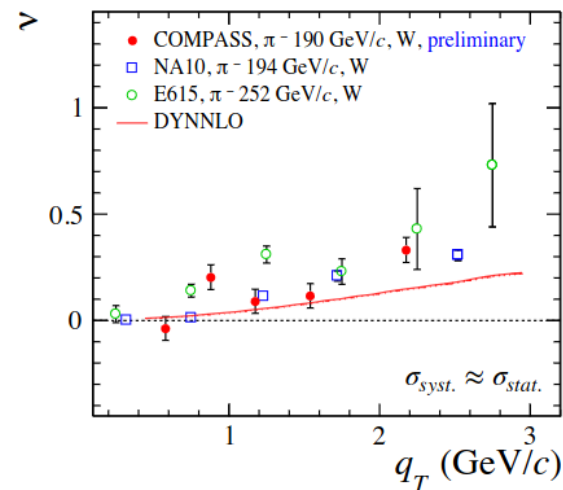
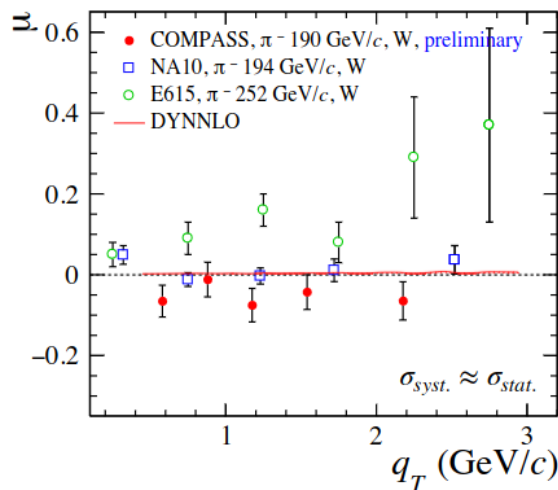
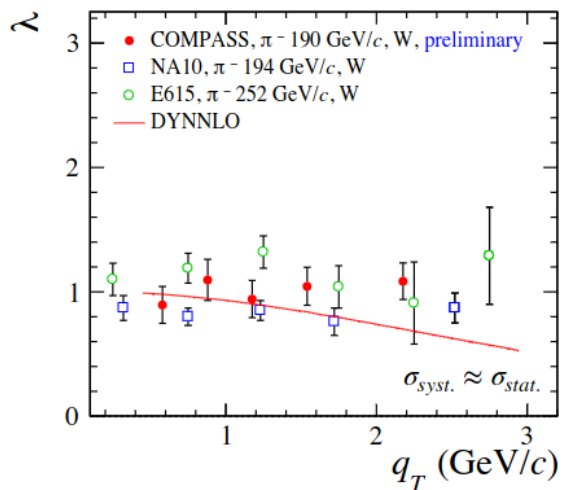


$$A_U^{\cos 2\varphi_{CS}} \propto h_{1,\pi}^{\perp q} \otimes h_{1,p}^{\perp q}$$

**Convolution of the Boer-Mulders TMD PDFs of pion and nucleon**

- In the naive Drell-Yan parton model, expect  $\lambda=1$ ,  $\nu=\mu=0$  (LO)
- At NLO, there might be a non-zero  $\nu$  ( $\cos 2\phi_{CS}$  dependence)
- **Lam-Tung relation:**  $1 - \lambda = 2 \nu$

# Drell-Yan unpolarized asymmetries



The Boer-Mulders-related coefficient  $v$  tends to be larger than expected from pQCD

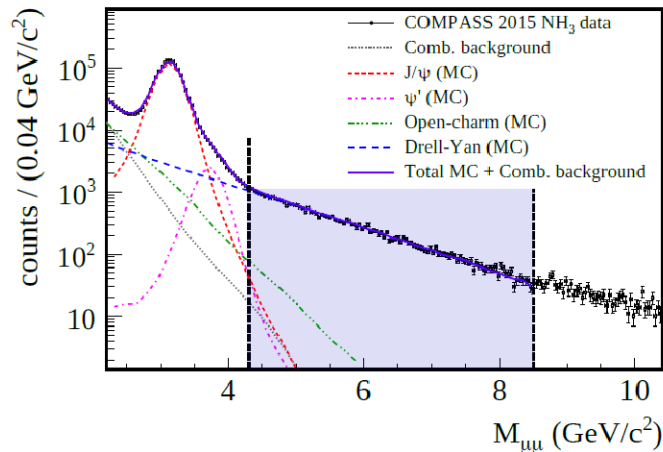


Hint for the presence of non-negligible Boer-Mulders effect

Possible violation of Lam-Tung relation.



# Differential Drell-Yan cross sections



$$\frac{d^n \sigma}{dx_n} = \frac{1}{\mathcal{L}} \times \frac{1}{\varepsilon} \times \frac{d^n N_{\mu\mu}}{dx_n}$$

$\mathcal{L}$  is the luminosity

$\varepsilon$  contains efficiencies, acceptance and lifetimes

$x_n$  are the different observables

The dimuon mass range  $4.3 < M_{\mu\mu}/(\text{GeV}/c^2) < 8.5$  is considered as Drell-Yan dominated.

Measurement of cross section requires good control of luminosity and efficiencies systematics.

For this reason, **only 2018 data** is used in the cross-section analysis.

Acceptance ranges from  $\sim 1\%$  to  $\sim 15\%$ .

It varies mostly with  $x_F$  (weak dependence with  $q_T$  and mass).

Contamination from other physics processes (purity) is taken into account.

$$\tau = M_{\mu\mu}^2/s = x_\pi x_N$$

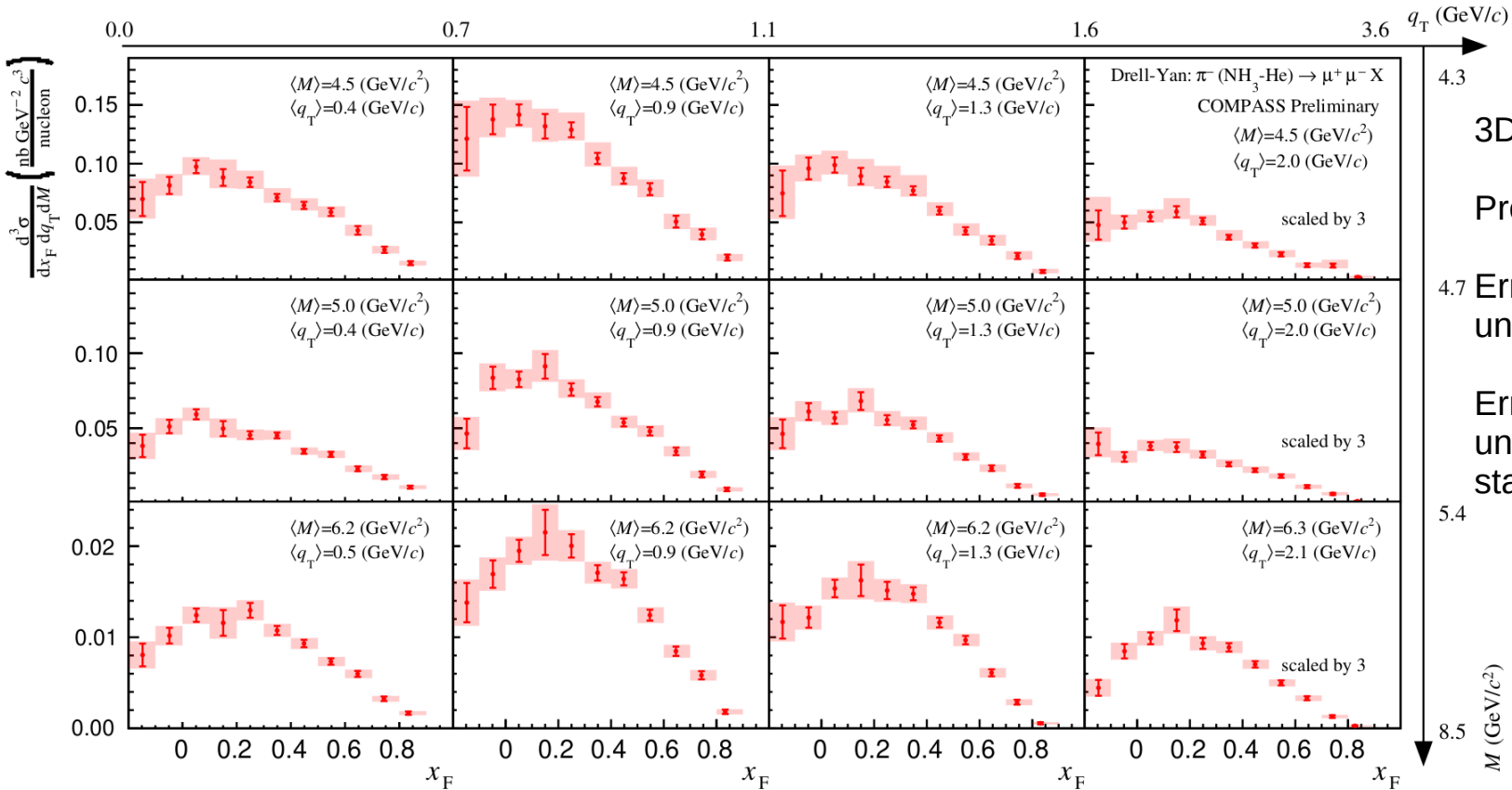
$\left. \begin{matrix} q_T \\ q_L \end{matrix} \right\}$  Transverse and longitudinal momentum of the dimuon in the Hadrons collision frame

$$x_F = q_L/(\sqrt{s}/2)$$

$$x_\pi = [x_F + \sqrt{x_F^2 + 4\tau}]/2$$

$$x_N = [-x_F + \sqrt{x_F^2 + 4\tau}]/2$$

# Drell-Yan cross section per nucleon from the ammonia-mix target in bins of mass and $q_T$ , as function of Feynman- $x$



3D cross sections (  $M$ ,  $q_T$ ,  $x_F$  )

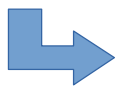
Preliminary results

4.7 Error bars are statistical uncertainty

Error bands are the total uncertainties (quadratic sum of stat. and syst. error)

5.4

8.5

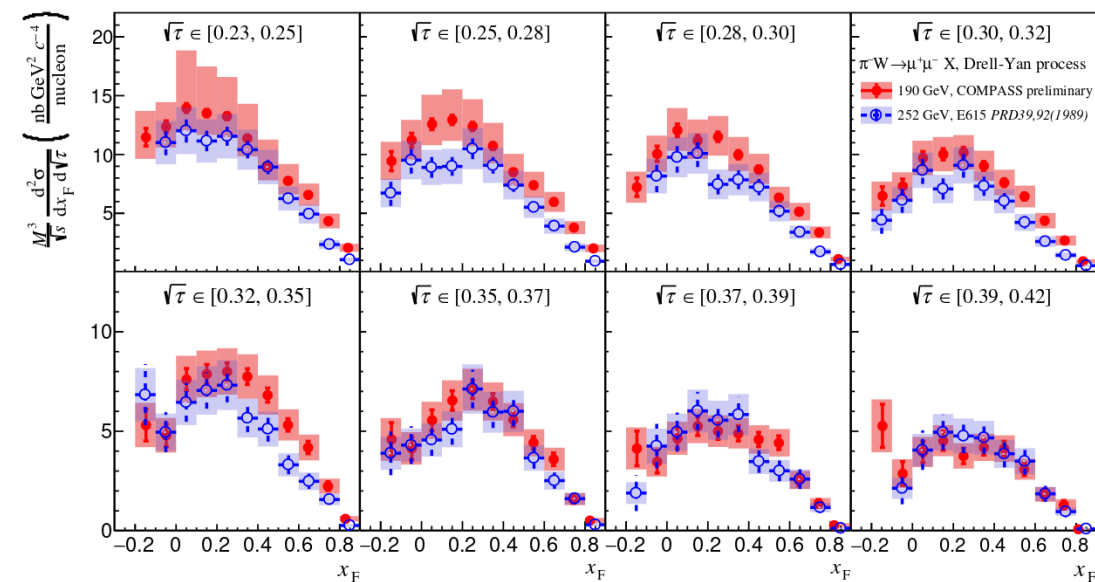


Input to global extraction of PDF and TMD PDF of the pion

# Drell-Yan cross section per nucleon from the tungsten target in bins of $\sqrt{\tau}$ , as function of Feynman-x



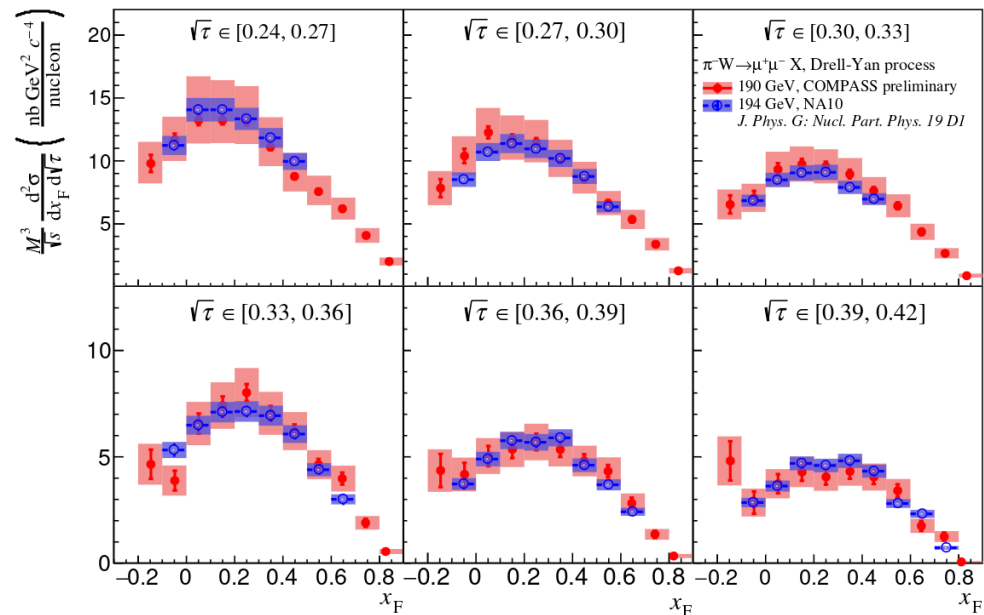
## COMPASS versus E615



E615 coll., Phys. Rev. D 39, 92-122 (1989)

$$\sqrt{\tau} = M/\sqrt{s}$$

## COMPASS versus NA10



NA10 coll., Z. Phys. C 28, 9 (1985)

Beam energy-independent DY cross section:  $M^3/\sqrt{s}$  factor

Better agreement with NA10 than with E615,  
namely at lower masses.

# Drell-Yan cross section statistics and systematics

The systematics of the COMPASS measurement include:

- Luminosity uncertainty  $\sim 4\%$  (normalization uncertainty)
- Trigger, purity and acceptance-related uncertainties depending on target and kinematics

		Statistics (#events)	Systematic uncertainty	#datapoints in $(M, x_F)$
COMPASS	NH3-He	36000	$\sim 5\%$	110
	Al	6000	$\sim 15\%$	50
	W	43000	$\sim 15\%$	50
NA10	W	155000	6.5%	59
E615	W	36000	16%	168

Ongoing work to evaluate the fraction of correlated and uncorrelated systematics.

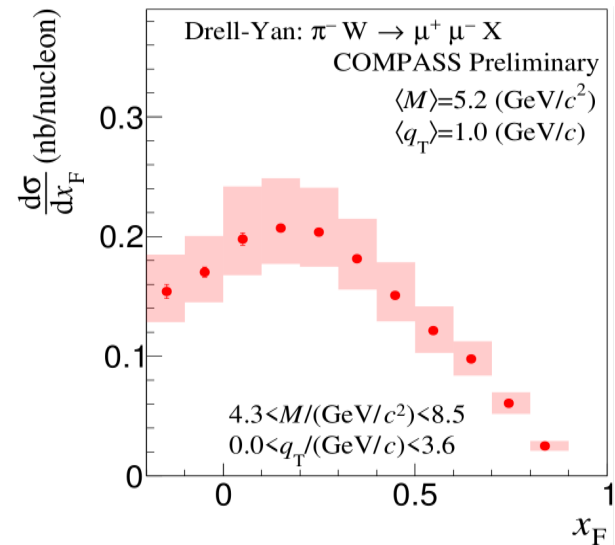
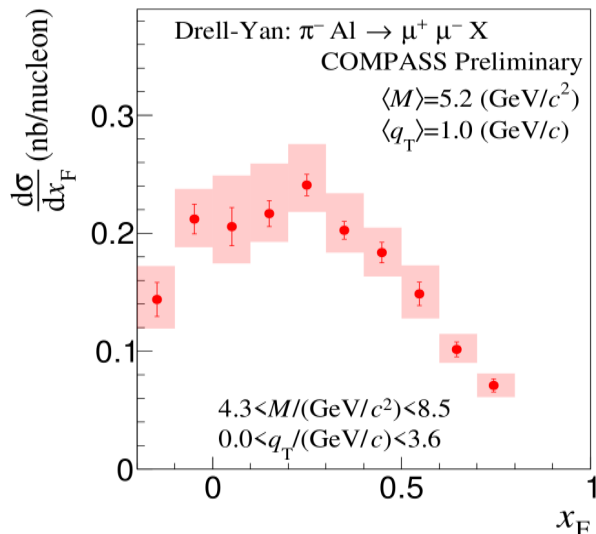
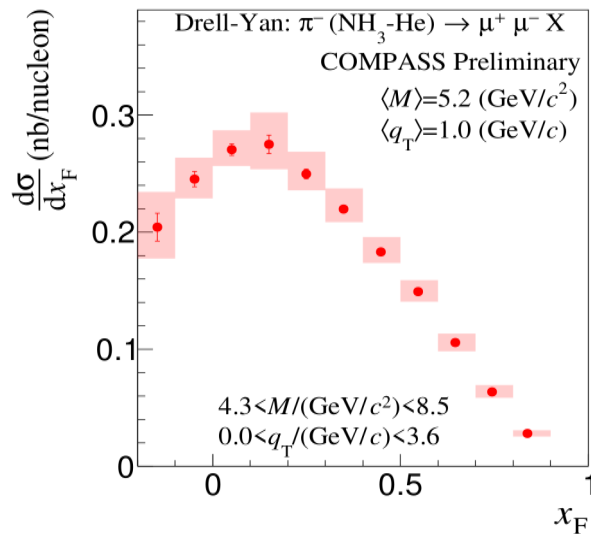
# Drell-Yan cross section per nucleon as a function of Feynman-x



**NH<sub>3</sub>-He**

**Al**

**W**



Preliminary results. Error bars are the statistical uncertainties.  
Error bands are the total uncertainties (quadratic sum of stat. and syst. error)



Input for the extraction of nuclear PDFs and study of nuclear effects

## From COMPASS to AMBER



COMPASS is providing much-awaited pion-induced Drell-Yan data (after a gap of 30 years).

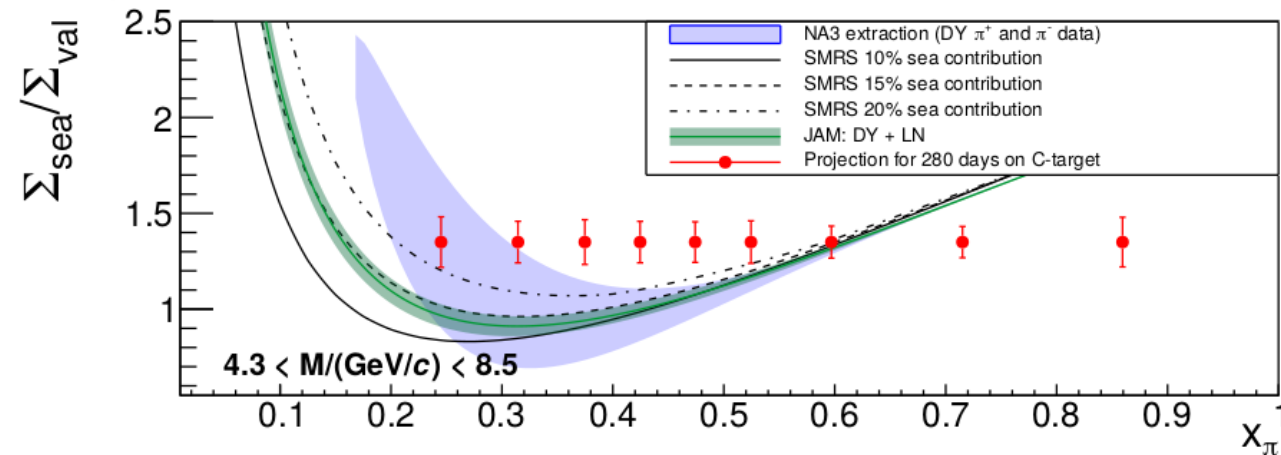
At COMPASS Drell-Yan, mostly **valence quarks** are probed – **u-quark dominance**, since  $\pi^-$  beam.

AMBER is the next step to learn about pion structure:

- Pion beam of both charges → **sea-valence separation**
- Benefit from the gained experience at COMPASS:
  - Light isoscalar target: **carbon**
  - Thinner and isolated **tungsten** target
  - Beam particle identification: CEDARs at beam high intensity
  - Improve vertexing and resolutions: vertex detector
  - Triggerless DAQ, with higher-level dimuon trigger – including online trigger efficiency control



## Future: $\pi$ -induced Drell-Yan with both beam charges



Valence composition:

$$u_{val}^{\pi^+} = u^{\pi^+} - \bar{u}^{\pi^+} \text{ and } d_{val}^{\pi^-} = d^{\pi^-} - \bar{d}^{\pi^-}$$

Flavour symmetry:

$$u_{val}^{\pi^+} = \bar{d}_{val}^{\pi^+} = \bar{u}_{val}^{\pi^-} = d_{val}^{\pi^-}$$

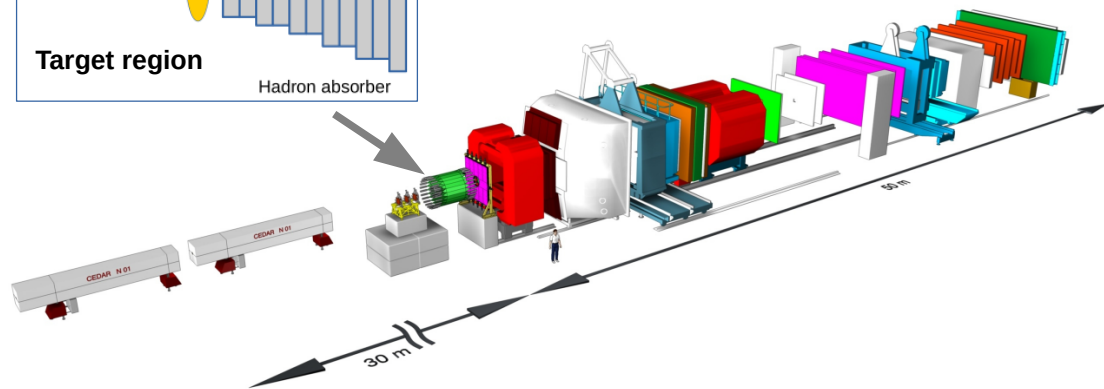
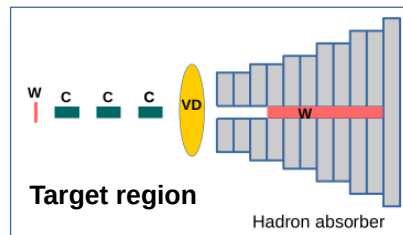
$$\bar{u}_{sea}^{\pi^+} = u_{sea}^{\pi^-} = \bar{d}_{sea}^{\pi^+} = d_{sea}^{\pi^-} = \bar{s}_{sea}^{\pi^+} = s_{sea}^{\pi^-}$$

Sea/valence separation (LO) from ratio of cross-section combinations:

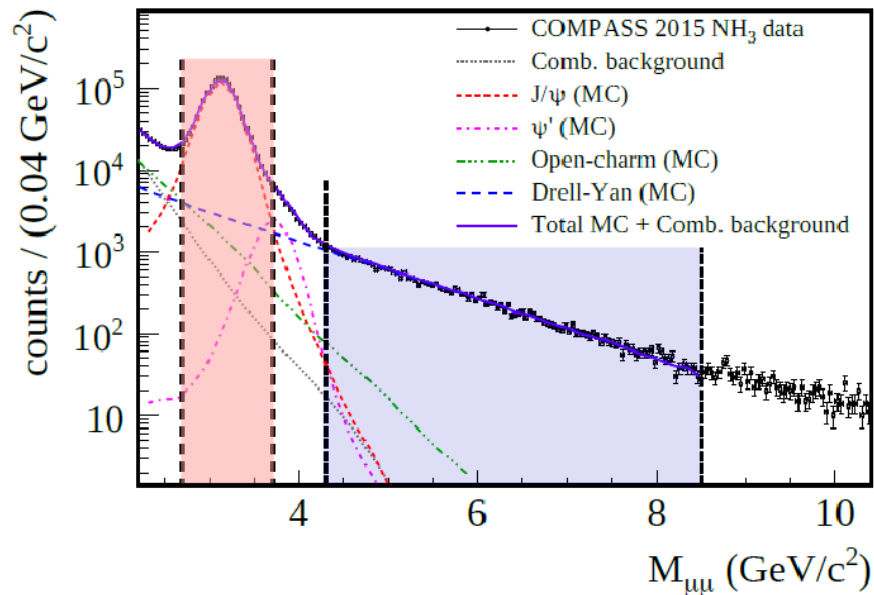
$$\frac{\Sigma_{sea}}{\Sigma_{valence}} = \frac{4\sigma^{\pi^+C} - \sigma^{\pi^-C}}{-\sigma^{\pi^+C} + \sigma^{\pi^-C}}$$

LO: only sea-val  
and val-sea terms

LO: only val-val terms



# Hadro-production of charmonium in COMPASS



$J/\psi$  and  $\psi(2S)$  data collected simultaneously with Drell-Yan.

Due to the limited mass resolution,  $\psi(2S)$  is hardly visible.

Due to the presence of hadron absorber, only access inclusive charmonium production.

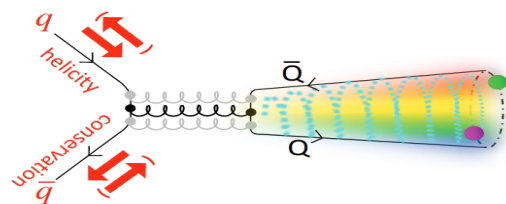
$$\pi^- A \rightarrow J/\psi X \rightarrow \mu^+ \mu^- X$$

$J/\psi$ -related analyses in COMPASS:

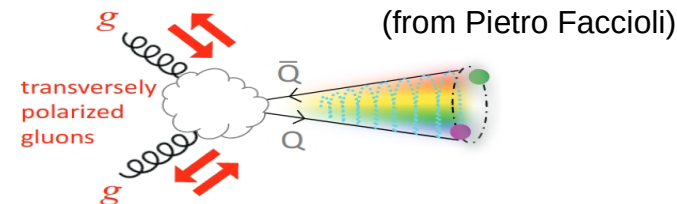
- Transverse spin asymmetries
- Unpolarized asymmetries (not yet released)
- Differential cross sections
- $J/\psi$ -pair production



# Charmonium production mechanisms



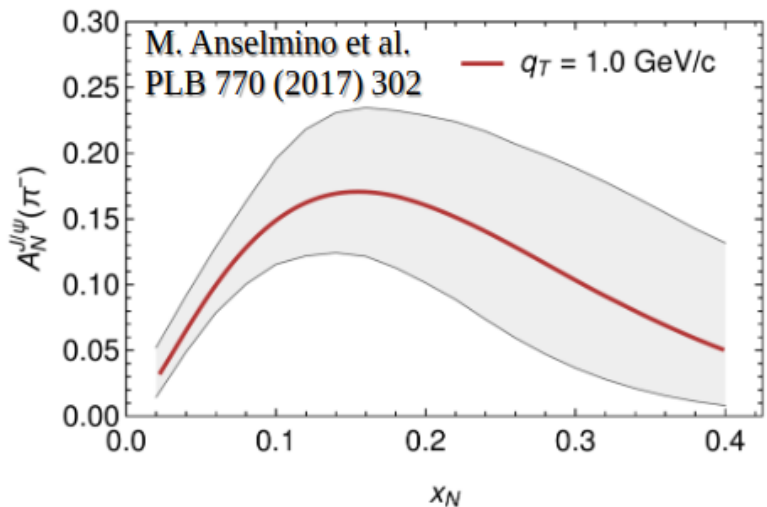
**$q\bar{q}$  annihilation**



**gluon-gluon fusion**

...and also  $qg$  contributions possible.

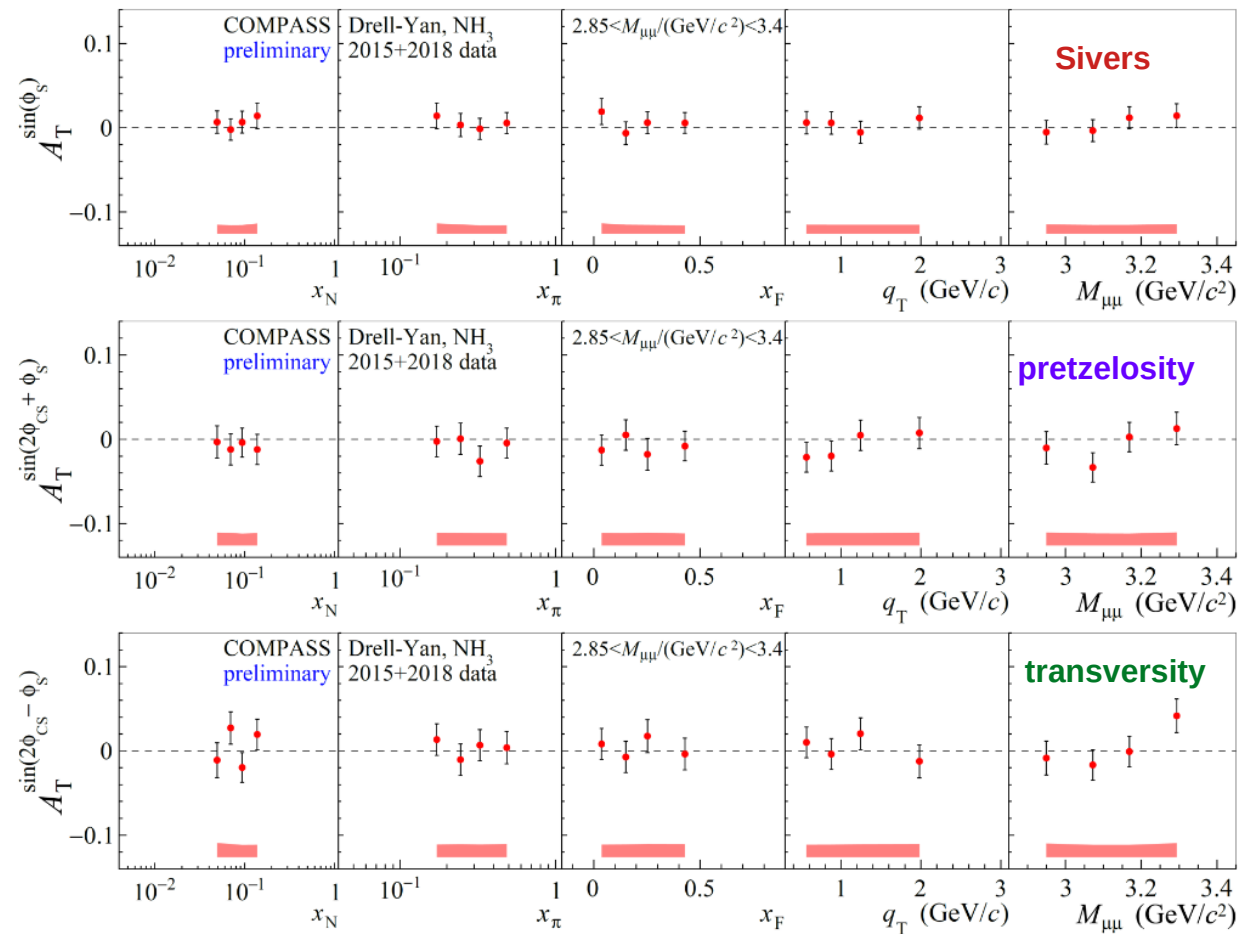
At COMPASS energies, the  $q\bar{q}$  mechanism is expected to contribute significantly, while at LHCb gluon-gluon fusion is dominant.



Assuming  $q\bar{q}$  annihilation dominance,  
M. Anselmino et al, PLB 770 (2017) 302

predicted large  $J/\psi$  transverse spin asymmetry and  
sensitivity to u-quark Sivers TMD PDF of the nucleon.

# Transverse spin asymmetries in the $J/\psi$ mass range



$J/\psi$ -dominated dimuon mass interval:

$$2.85 < M_{\mu\mu}/(\text{GeV}/c^2) < 3.4$$

Lower  $\langle x_N \rangle$  and  $\langle x_\pi \rangle$  as compared to high mass Drell-Yan

Worse position resolution as compared to high mass Drell-Yan – small leakage from one cell into another.

➡ All TSAs compatible with zero

# Study of “cold nuclear matter” effects



Different phenomena observed. At low  $x$  driven by partons multiple scattering.

A useful observable is the **Nuclear modification factor:**

If no nuclear effects:  $R_{hA} = 1$

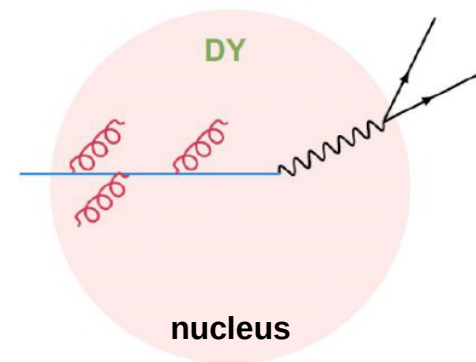
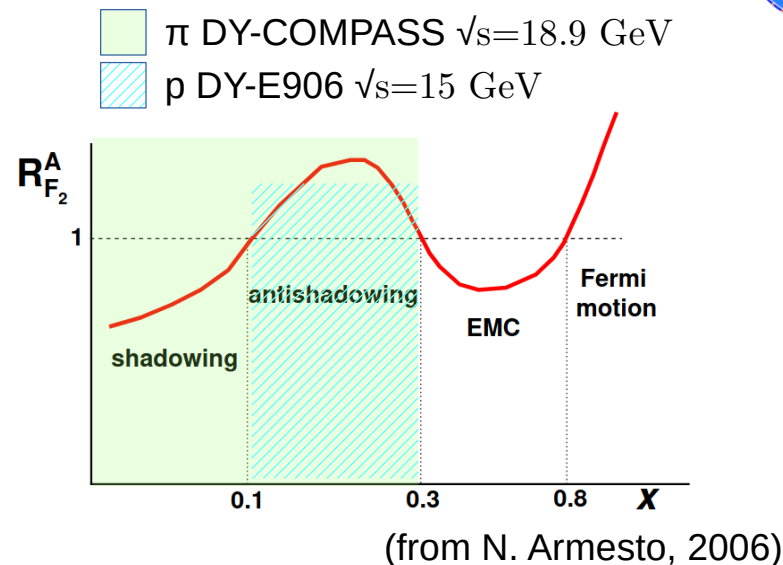
$$R_{hA} = \frac{dN_{hA}^{J/\psi}}{\langle N_{coll} \rangle dN_{hh}^{J/\psi}}$$

Try to encode it all in process-independent **nPDFs**

Partons may also lose energy via soft gluon emissions when crossing the cold nuclear matter

Different hard processes allow to study the **energy loss effect:**

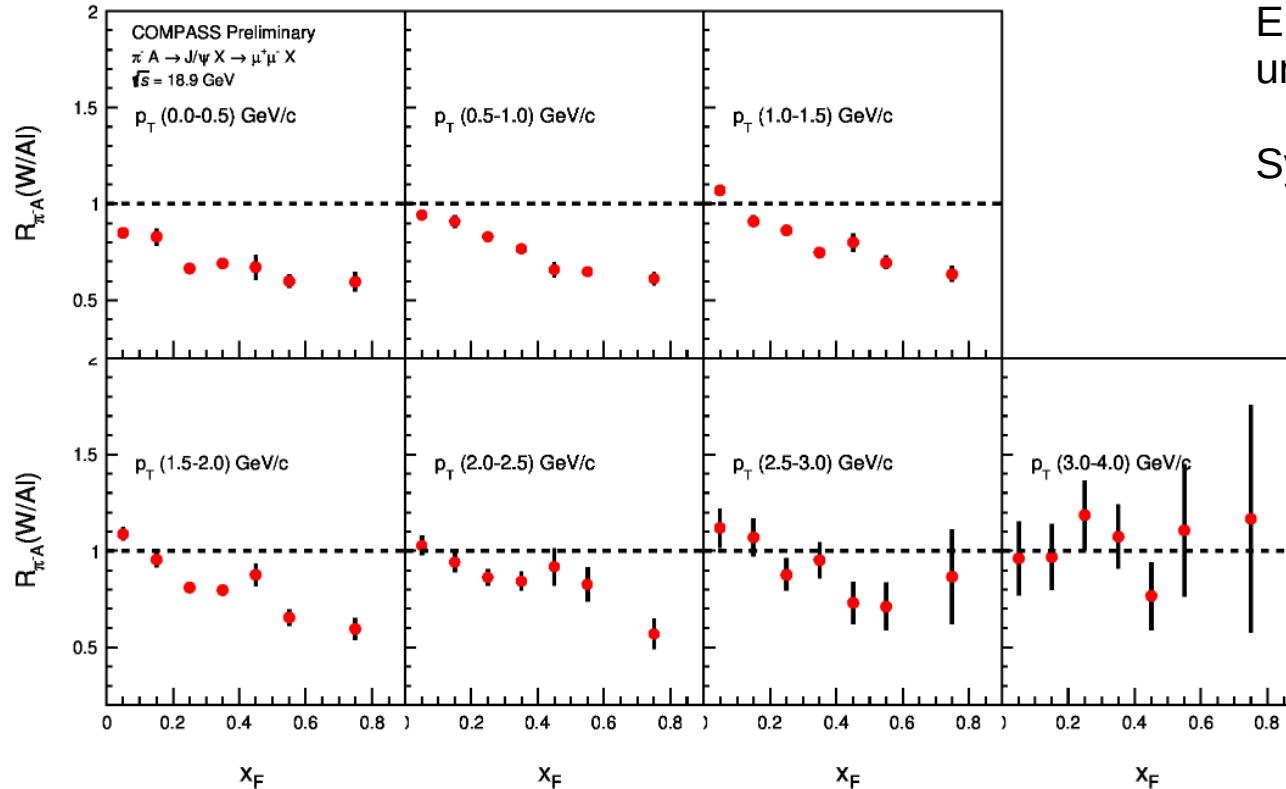
- **Drell-Yan** → initial state radiation
- **$J/\psi$  production** → initial and final state radiation, interference



# J/ψ production cross-section ratios



$R_{\pi A}(W/Al)$  ( $x_F$ ,  $p_T$ ) : ratio of J/ψ production cross sections per nucleon between W and Al targets in ( $x_F, p_T$ ) bins.



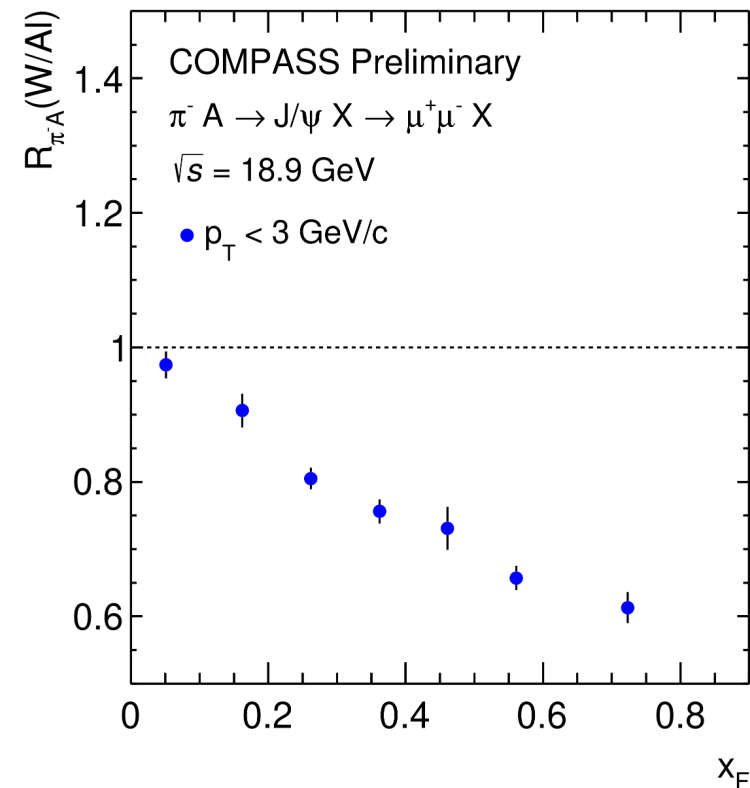
Error bars show the statistical uncertainty.

Systematic uncertainty <10%

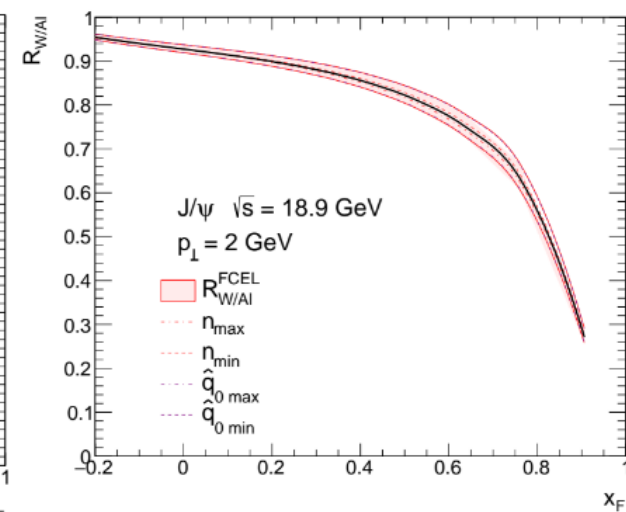
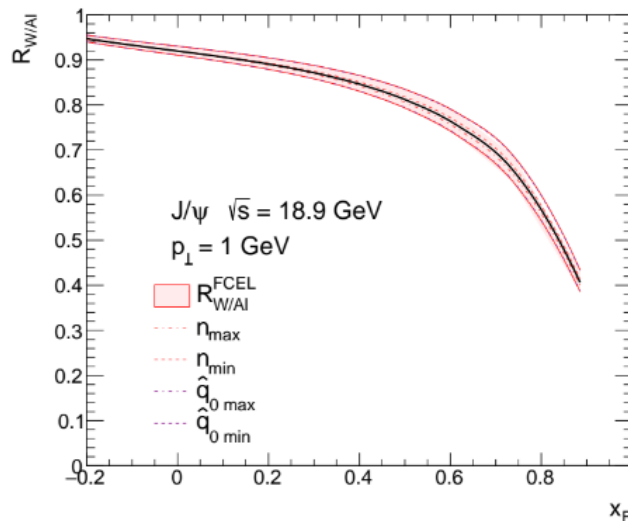
Suppression towards high  $x_F$ , more prominent at low  $p_T$ .

This 2D analysis provides additional insight, not possible from past experiments.

# J/ψ nuclear modification factor and parton energy loss



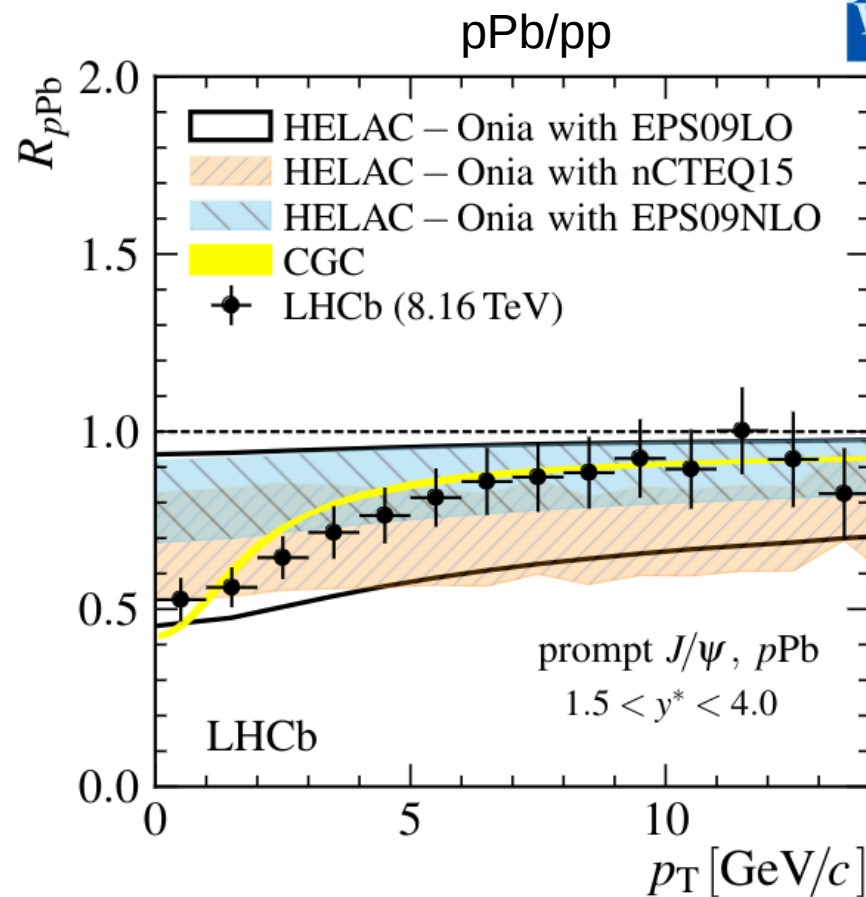
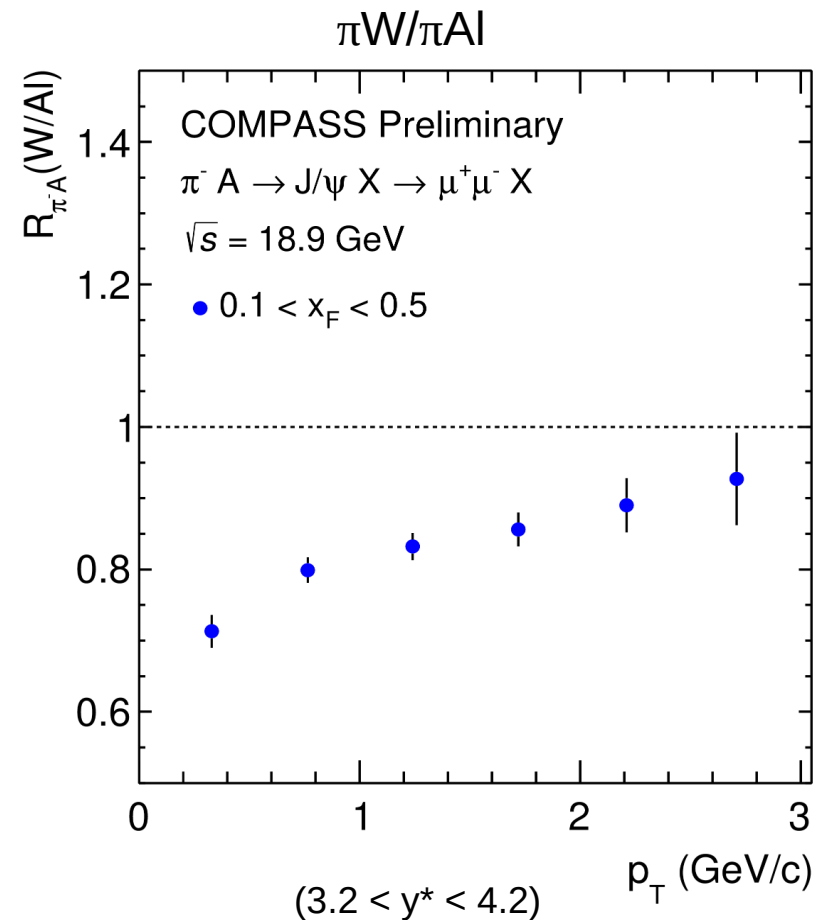
Using a **model of energy loss**, with transport coefficient  $q_0$ , by F. Arléo and S. Peigné, as in JHEP 03 (2013) 122.



F. Arléo, private communication, preliminary

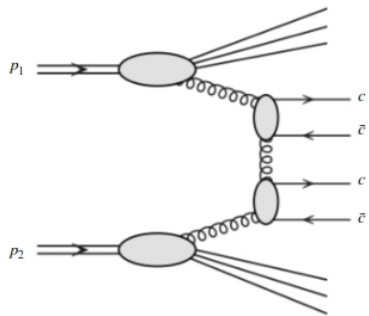


# J/ $\psi$ nuclear modification factor: Comparing to LHCb



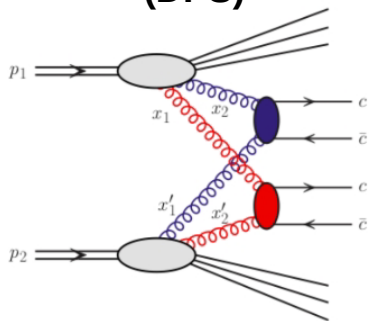
LHCb, PLB 774 (2017) 159-178

## Single parton scattering (SPS)



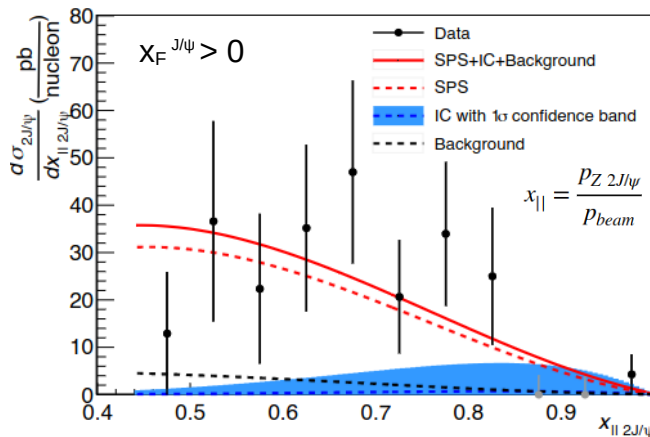
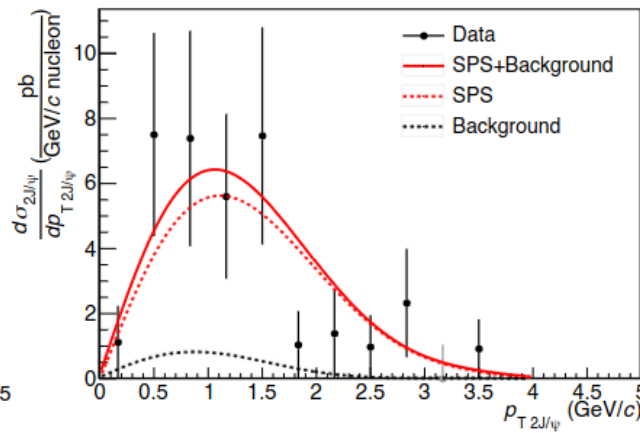
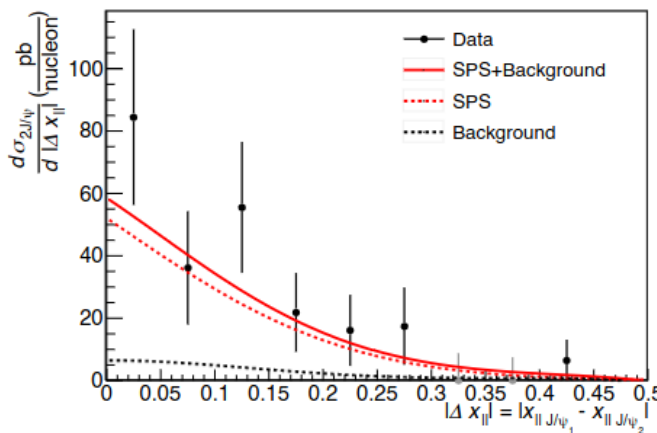
SPS expected to dominate at COMPASS energies

## Double parton scattering (DPS)



## J/ψ pair production

COMPASS, PLB 838 (2023) 137702



COMPASS results are consistent with pure SPS hypothesis

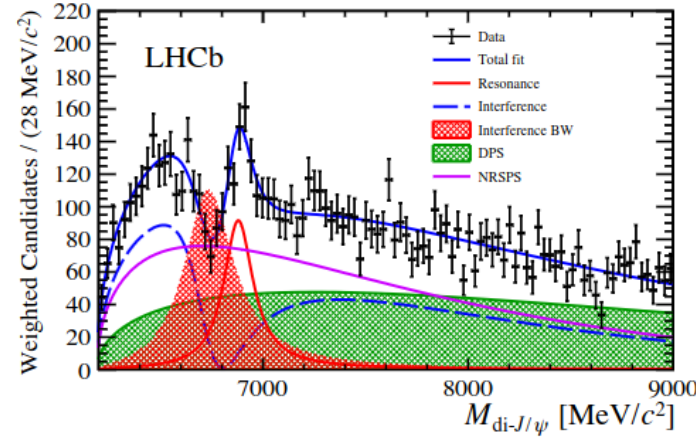
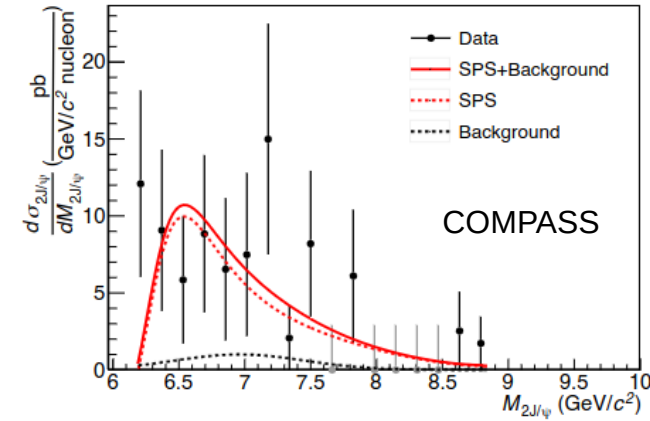
An upper limit on **intrinsic charm** (IC) production mechanism is obtained:

$$\sigma_{2J/\psi}^{IC} / \sigma_{2J/\psi} \Big|_{x_F > 0} < 0.24 \text{ (CL = 90\%)}$$

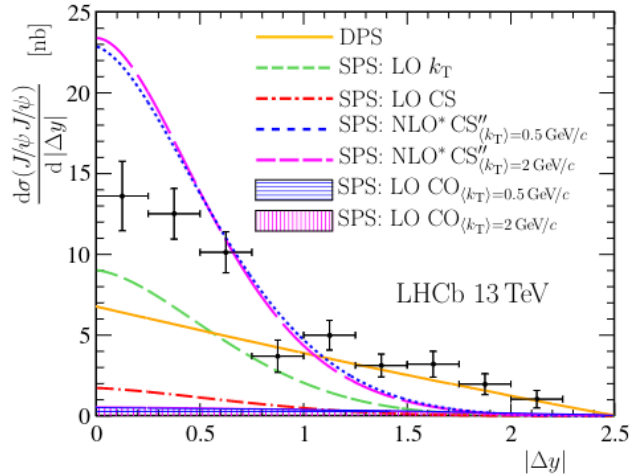
# J/ψ pair production



COMPASS, PLB 838 (2023) 137702



COMPASS sees no evidence for the exotic state reported by LHCb, *Sci. Bull.* 65 (2020) 1983-1993



$$M[X(6900)] = 6886 \pm 11 \pm 11 \text{ MeV}$$

$$\Gamma[X(6900)] = 168 \pm 33 \pm 69 \text{ MeV}$$



Enhanced contribution of DPS at LHC energies allows LHCb to separate SPS and DPS in J/ψ pair production  
LHCb, JHEP 06 (2017) 047.

J/ψ pair production from isolated SPS contribution



access to the **gluon TMD PDFs**

Modulations extracted are so-far consistent with zero  
LHCb, JHEP 03 (2024) 088



## In summary:

- COMPASS studied for the first time the transversely polarized Drell-Yan process, collecting data in 2015 and 2018.
- The measured Sivers asymmetry in Drell-Yan is compatible with the [sign-change hypothesis](#) with respect to SIDIS, (also measured in COMPASS).
- The [pion-induced Drell-Yan cross section](#) is measured from the 2018 data, in a multidimensional analysis ( $M$ ,  $q_T$ ,  $x_F$ ).
- Visible hint for a [non-zero Boer-Mulders effect](#) in the angular dependence of the Drell-Yan cross section.
- [Inclusive  \$J/\psi\$  production](#) is studied in parallel. All measured transverse spin asymmetries are compatible with zero.
- Evidence for [cold nuclear matter effects](#), visible in the  $J/\psi$  cross-section ratio  $W/A$ .
- [\$J/\psi\$  pair production in COMPASS](#) is measured to be compatible with [pure SPS contribution](#).
- No evidence in COMPASS for the  $X(6900)$  exotic previously observed by LHCb.





## Conclusion



Good harvest of results from the COMPASS Drell-Yan campaign.

Most of these are not yet published → publications should follow soon!

Learning curve getting steeper, with many ideas on how one could improve experimentally → AMBER

SPARES

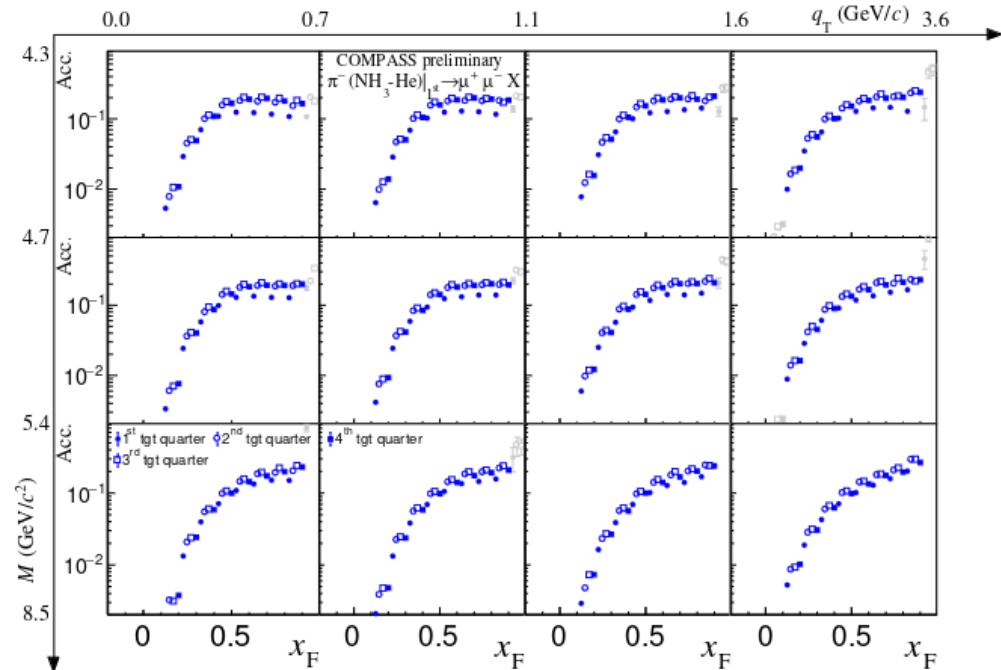
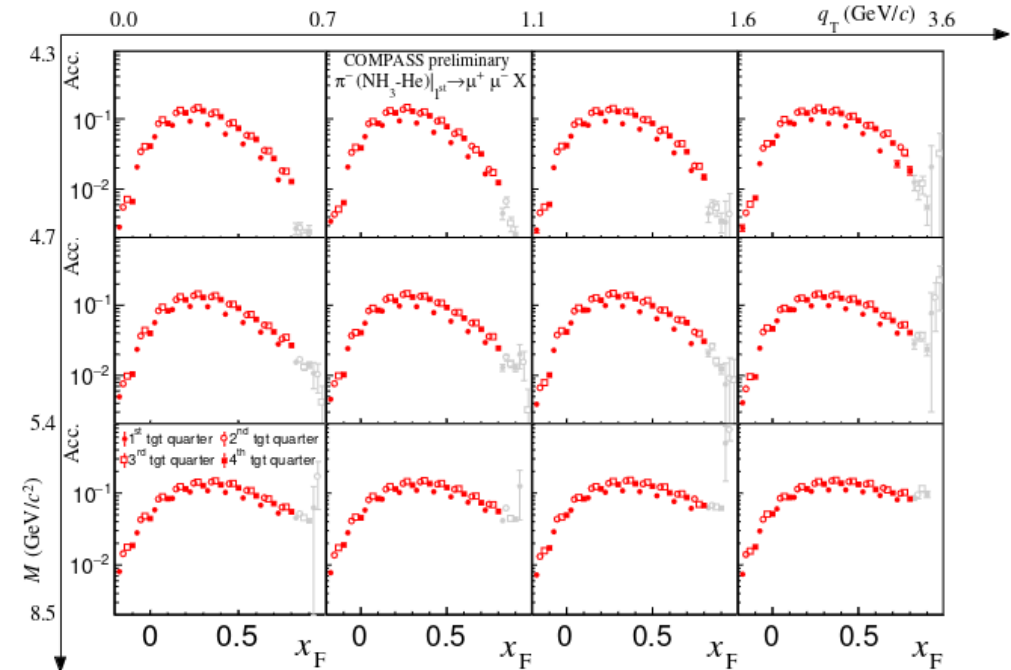
# High mass Drell-Yan Acceptance

Evaluated in 4 dimensions ( $M$ ,  $q_T$ ,  $x_F$ ,  $Z_{\text{vertex}}$ ) and separately per dimuon trigger

Example: ( $\text{NH}_3$ -He) target

**LAS-LAS**

**LAS-OUTER**



Measurement restricted to the range where the acceptance relative accuracy is better than 10%

Acceptance ranges from ~1% to ~15%

# Drell-Yan process purity

The DY purity in the mass range 4.3 – 8.5 GeV/c<sup>2</sup> is evaluated from a **cocktail fit** to the dimuon mass spectrum, and taken into account in the final cross section.

Study done in ( $q_T$ ,  $x_F$ ) bins, separately per target and trigger.

The purity is above 90% for:

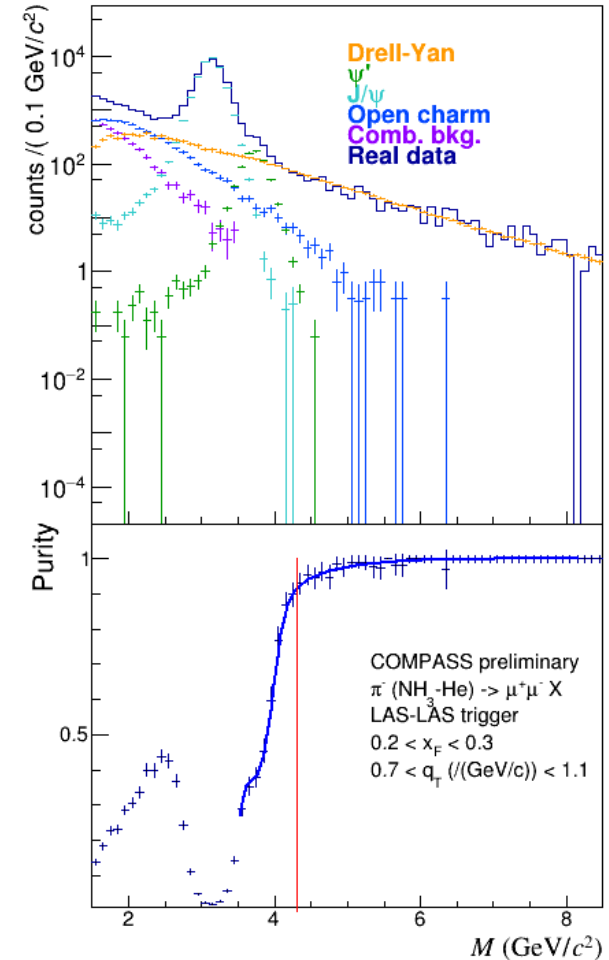
- NH3-He :  $M > 4.3$  GeV/c<sup>2</sup>
- Al:  $M > 4.7$  GeV/c<sup>2</sup>
- W:  $M > 5.5$  GeV/c<sup>2</sup>

The purity is affected by the mass resolution, worse for W.

The resolutions are also evaluated from Monte Carlo:

Target	$\delta x_F$	$\delta q_T$ (MeV/c)	$\delta M/M$
NH3-He	0.03	150	3.5%
He	0.03	245	4.5%
W	0.03	340	6.5%

Example:



# Drell-Yan cross section per nucleon, in bins of mass, as function of $q_T$



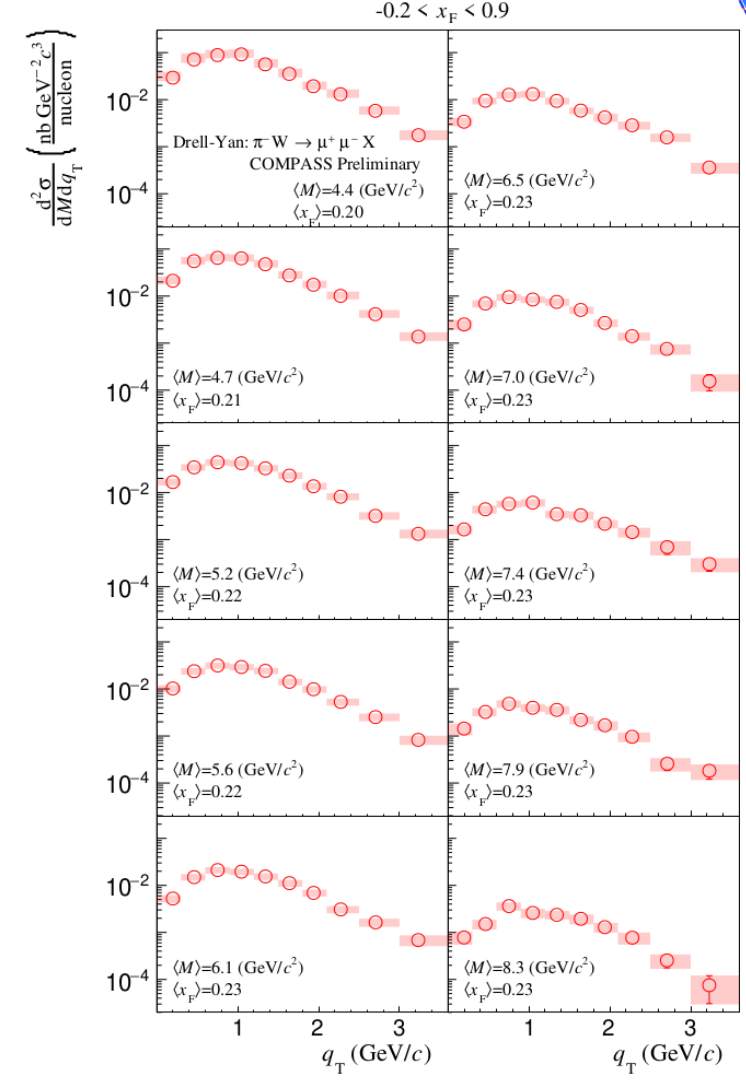
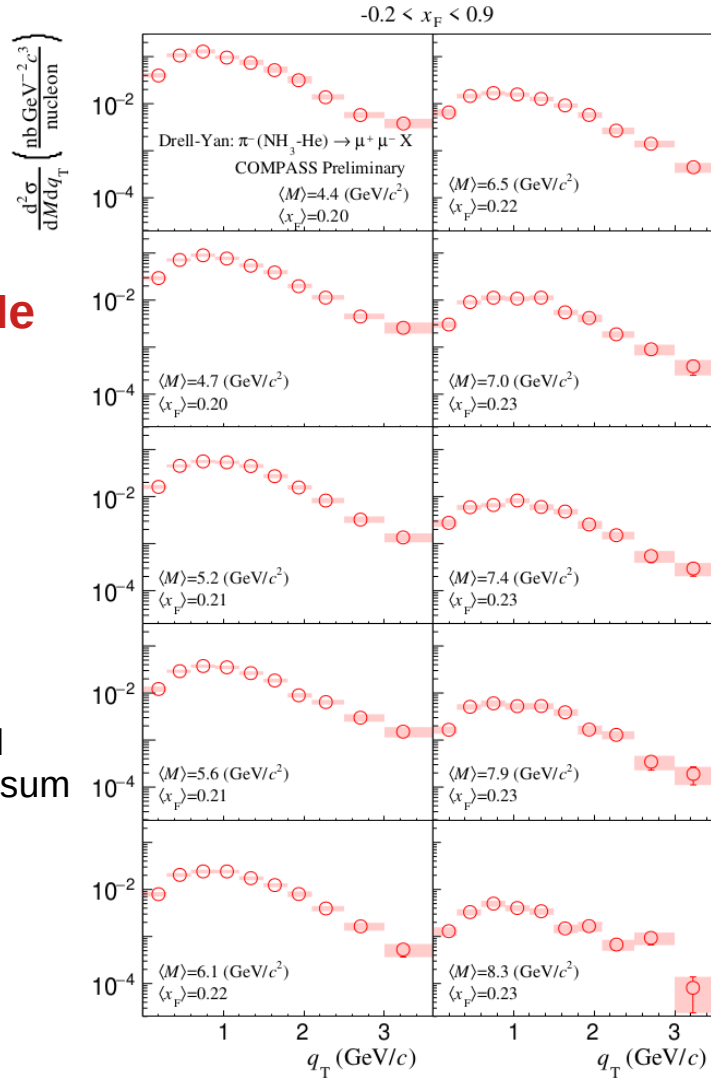
**NH<sub>3</sub>-He**

2D cross section ( $M, q_T$ )

Preliminary results

Error bars are statistical  
Uncertainty

Error bands are the total  
uncertainties (quadratic sum  
of stat. and syst. error)



**W**